Mon. Not. R. astr. Soc. (1991) **249**, 606–628

A uniformly selected catalogue of distant galaxy clusters

Warrick J. Couch,[1,3] Richard S. Ellis,[2] David F. Malin[3] and Iain MacLaren[2]

[1] *School of Physics, University of New South Wales, Sydney, NSW, Australia*
[2] *Physics Department, University of Durham*
[3] *Anglo-Australian Observatory, Epping, NSW, Australia*

Accepted 1990 November 5. Received 1990 October 22; in original form 1990 August 13

SUMMARY

We present a new catalogue of faint southern galaxy clusters identified from examination of high-contrast film derivatives of a set of 55 prime focus AAT photographic plates taken in one or both of two pass-bands ($J \equiv b_J$ and $F \equiv r_F$). Visual scans of these films have been compared with machine measurements of the original plates and the results demonstrate that the films offer ready access to the positions (but not photometry) of large numbers of faint objects to limiting magnitudes of $b_J \simeq 24.4 \pm 0.3$ and $r_F \simeq 22.9 \pm 0.2$. Our cluster candidates are chosen according to their *contrast*, $\sigma_{\rm cl}$, above the fluctuations in the field counts as determined locally on the same film. A total of 112 candidate clusters are tabulated down to a contrast level of $\sigma_{\rm cl} = 2.0$ (at which point marginal effects become apparent). Cross-correlations with published catalogues (and spectroscopic measurements) confirm that the bulk of these clusters are more distant than those found by Abell and co-workers. By applying our search criteria to simulated fields containing clusters of known richnesses, and with fluctuations in the field counts matching those seen in the data, we determine our cluster list should be complete above a limit $\sigma_{\rm cl} = 3.25$. Given recent estimates of the volume density of clusters of various richnesses, our simulations predict the observed number of F clusters seen above the $\sigma_{\rm cl} = 3.25$ limit, but predict too few J clusters. To test for the origin of this excess of blue clusters we have measured redshifts for 95 faint galaxies in 29 of the 44 clusters with $\sigma_{\rm cl} > 4.0$ using a variety of telescopes and instruments. A spectroscopically complete subsample in 16 fields allows us to determine the absolute space density. The spectroscopy confirms the reality of the clusters with $\sigma_{\rm cl} > 4.0$ and shows a redshift range for the F sample similar to that expected without luminosity or cluster evolution; the J sample extends to higher redshifts than expected. A detailed study of the highest redshift clusters suggests the abundance of high-redshift J clusters arises either from projections from foreground spiral-rich groups or via recent star formation within the distant cluster environments. In support of the latter hypothesis, we demonstrate how bursts of star formation in a subset of cluster galaxies would transform the J contrast leaving the F contrast largely unaffected – in agreement with the basic trend observed. We discuss the implications of our results for further searches for high-z clusters. Only with the advent of wide-field infrared imaging, or X-ray selected samples, might *galaxy-dependent* selection effects associated with variations in stellar populations at a given epoch be overcome.

1 INTRODUCTION

Galaxy cluster catalogues compiled from Schmidt telescope plate material – notably those of Abell (1958) and Zwicky *et al.* (1961–68) – have served as valuable resources in observational cosmology. Clusters are useful both as fundamental systems where sizeable populations of galaxies can be simultaneously observed, and as economic tracers of large-scale structure at diverse wavelengths. Although there have been various discussions as to the statistical complete-

ness of optically selected cluster catalogues (*cf.* Lucey 1983), there is no doubt that such compilations have provided useful collections of objects with a range of properties out to moderate distances ($z \sim 0.2$).

However, at distances beyond the limits of these Schmidt-based catalogues, inventories of clusters are scarce. Apart from the work of Gunn, Hoessel & Oke (1986, hereafter GHO), who concentrated on six specific northern fields, there has been no systematic deep cataloguing of clusters over large areas of sky. Consequently, workers have been obliged to use whatever clusters have been reported in the literature – a dangerous practice given the heterogeneity of the selection methods used (involving studies at radio and X-ray, as well as optical, wavelengths).

Since the advent of hydrogen hypersensitizing in 1974, many deep, fine-grain, high-resolution plates have been obtained at the prime foci of the newer 4 m class telescopes. Whilst the target fields have not normally been chosen randomly, the wide angle correctors of these instruments ensure that each plate records a substantial area of the sky around the intended object. The faintest images on these plates are substantially fainter than those obtained from Schmidt sky surveys on similar photographic emulsions. Prompted by the improvements in photographic materials, novel photographic image enhancement techniques have been developed to improve the qualitative detection of low-surface-brightness objects. At the same time, plate measuring machines have been constructed which provide quantitative information at faint limits. Motivated by the need for a systematic survey of clusters at these depths and our own interest in using galaxies in distant clusters as probes of evolution, we have constructed a new catalogue of *southern* clusters using as our basic source material an archive of high-quality sky-limited plates taken on the 3.9 m Anglo–Australian Telescope (AAT) since its commissioning in 1975.

This southern catalogue, which might be conveniently called the *AAT Deep Cluster Catalogue*, has been referred to in a number of earlier papers and review articles (Couch *et al.* 1984; Ellis 1987, 1988; Couch, Ellis & Malin 1989). Although the source catalogue was constructed several years ago (MacLaren 1987), gathering the spectroscopic measurements in order to determine a redshift for even a subset of the clusters has consumed many nights of telescope time and hence taken several years to complete. This paper summarizes both the criteria adopted in constructing the source catalogue and our strategy for the associated spectroscopy. It also presents the complete catalogue of clusters.

Fundamental to our search has been the production by Malin of *high-contrast* film copies of each plate. This technique, tests of its applicability, and the selection criteria used in finding the clusters are described in Section 2. In Section 3 we develop basic models for predicting the surface density of clusters expected on the basis of local samples. In Section 4 we then discuss the redshift measurements obtained for a subset of our catalogue, both to verify the reality of the clusters and to determine their redshift range for comparison with the models above. Finally, in Section 5 we discuss the implications of our cluster data in terms of constraints on evolution, both in the volume density of clusters and in possible colour/luminosity evolution of their constituent galaxies, and discuss the prospects for finding clusters at higher redshifts by various techniques. Our conclusions are summarized in Section 6.

2 METHODS AND SELECTION CRITERIA

2.1 Photographic material

The basic photographic material for this search consists of 55 photographic plates taken at the $f/3.3$ prime focus of the 3.9 m Anglo–Australian Telescope (AAT) during the period 1977–82. Virtually all plates taken at the AAT, regardless of the scientific programme, are copied by Malin at two levels of contrast, and the resulting films kept in an archive at the AAO. The selection of films used for this project was based on the following criteria for the original plates.

(i) The plates had to be taken in one of two standard passbands: Kodak IIIa J + Schott GG 385 (hereafter J) and Kodak IIIa F + Schott RG 630 (hereafter F); plates taken in U, B, I or through non-standard filters were discarded in order to maintain homogeneity. Most plates were taken with the triplet corrector which provides an unvignetted field of about 1° diameter and a plate-scale of 15.3 arcsec mm^{-1}. A few plates were taken with a doublet corrector which has an unvignetted field of 40 arcmin diameter and a scale of 16.4 arcsec mm^{-1}.

(ii) The exposures had to be *sky-limited* – typically 50 min in F, 80 min in J. A sky-limited exposure is one where the sky photographic density typically reaches $D \sim 0.8$ above chemical fog.

(iii) The atmospheric seeing as measured from stellar images on the plate had to be better than 2 arcsec FWHM.

Of course such criteria do not guarantee that *each plate* has the same limiting magnitude; such homogeneity would be impossible to maintain without calibrated photometry even if the plates had been taken specifically for this programme. Within some limits the surface density of galaxies counted per unit area on each plate gives an indication of the degree of homogeneity. Together with comparisons on those few plates where CCD-calibrated photometry is available, an indication of the depths reached in such sky-limited exposures can readily be determined (see also discussion in Couch *et al.* 1984). We demonstrate below that likely variations in such limiting criteria do not grossly affect the visibility of clusters (see Section 3).

All of the photographic plates used in this programme were originally taken for unrelated scientific programmes and thus there is a wide range of field centres. This contrasts with the programme of GHO where plates were specifically taken for a distant cluster search in a few small selected areas. Recent redshift surveys (Koo & Kron 1988; Broadhurst *et al.* 1990) have provided growing evidence that rich cluster positions may be strongly correlated on large scales. If so, a more representative distribution of cluster redshifts is likely in a search centred on many random centres, rather than in a few large areas composed of contiguous fields. In practice most of the AAT plates are centred either on blank fields (for galaxy count programmes) or on bright (< 15.0 mag) galaxies where there should be no obvious bias in terms of a faint cluster programme. A few fields are centred on moderate-redshift ($z \sim 0.15$–0.2) clusters and we naturally take this into account in our statistical analysis.

2.2 The high-contrast technique

It would be very laborious to photometrically calibrate 55 photographic plates, and digitize each with a measuring machine, in order to construct a photometric catalogue from which clusters could be identified. The novel aspect of our search procedure is based on successful tests conducted with high-contrast film derivatives (HCFs) of a few plates. In these tests, catalogues based on both visual and measuring machine scans of these *films* were compared with genuine photometric catalogues based on COSMOS machine (Stobie *et al.* 1979) scans of the original glass photographic plates from which the films were derived.

Following the successful outcome of these tests, which we review below, we chose to survey HCFs (which were produced for each of the 55 AAT plates) visually for faint clusters using a well-defined procedure detailed in Section 2.3. In identifying faint clusters, we demonstrate in Section 3 that the most important criterion is the *contrast* in galaxy counts within some radius as compared to the background population; photometric information is less critical. The speed with which large areas of sky can be visually searched to very faint limits using wide-field HCFs makes this technique a most powerful method for finding weak enhancements.

The high-contrast technique, which conveniently increases the visibility of faint features, especially extended objects of low surface brightness, has been described by Malin (1978). The technique consists of preparing a high-contrast but low-density contact copy of the plates on a high-contrast film using a diffuse light source. From these positives, even contrastier contact (i.e. same scale) negatives are made. These negatives reveal objects that are often too faint to be seen by eye on the original plates. Tests of the applicability of searching these films for enhancements in the surface distributions of galaxies are discussed by both Couch *et al.* (1984) and MacLaren (1987), and here we present a brief summary of the results found.

Couch *et al.* (1984) compared the results of a visual search for faint objects on a single HCF with APM scans (Kibblewhite 1980) of both the original AAT glass negative plate and the negative film itself. They determined that eye searches of the HCF, tabulated independently by three observers and subsequently collated, found virtually all the objects to $b_J = 24.5$ in the APM catalogue with no incompleteness to this limit. Remarkably, however, the HCF catalogue as provided by each of the three observers probed somewhat deeper, and a subsequent CCD image of a subset of the area confirmed that virtually *all* of the 'extra' objects found by eye on the HCF but not present in the APM catalogue were, in fact, *bona fide* objects. The actual limiting magnitude of the HCF catalogue on that particular plate was between $b_J = 24.5$ and 25.0. The plate selected for this experiment, J1888, was centred exactly at the South Galactic Pole, and was one used by Shanks *et al.* (1984) for a galaxy count programme. It also contains a cluster J1888.16CL with redshift $z = 0.57$, which was found as part of our survey, but is discussed independently by Couch *et al.* (1985).

This APM versus HCF comparison was done prior to the bulk of the cluster searching discussed in this paper. To check whether the comparison is representative of other plates, MacLaren (1987) examined a further plate, this time comparing his HCF catalogue with CCD-calibrated photometry obtained using the COSMOS machine. In this second comparison using a high-latitude plate, J1836, as before the agreement to $b_J = 24.5$ was excellent. However, both catalogues probed beyond $b_J = 24.5$ in this case (in contrast to the corresponding APM catalogue on the earlier comparison), and MacLaren's comparison revealed some discrepancies at the fainter magnitudes. Beyond $b_J = 24.5$, an increasing number of objects is found by COSMOS which are *not* identified by eye on the HCF. Furthermore, a large number of HCF objects are present on the HCFs which the COSMOS scans failed to detect.

A deep CCD frame of a subset area revealed, however, that almost all (17 out of 19) of the excess objects found by eye on the HCF but not by COSMOS are present on the CCD frames. This confirms that these are indeed genuine objects and not spurious effects introduced by the HCF technique or produced as a result of the subjective nature of the visual searches. However, the objects that were detected only by COSMOS fainter than $b_J = 24.5$ are generally *not* present in the CCD catalogue, where a comparison is possible, and must therefore be spurious. Furthermore, in densely clustered areas there is also a danger of merging adjacent images in the machine measured catalogues. Also, bright images are often fragmented into large numbers of fainter sources. Both effects would make automatic detection of faint clusters very unreliable.

Remarkably, therefore, rather than being deficient compared to the measuring machines, the HCF technique actually *outperforms* both COSMOS and APM *in the detection* rather than photometry, of faint features. Eye scanning the films is also considerably more efficient. The statistics of both the Couch *et al.* and MacLaren comparisons are summarized for convenience in Table 1.

Table 1. HCF versus measuring machine comparisons.

	Number of objects found by :			
b_J	COSMOS	COSMOS and HCF	COSMOS and not HCF	COSMOS and CCD
23.50–24.00	31	30	1	1
24.00–24.25	14	12	2	0
24.25–24.50	19	17	2	1
24.50–24.75	21	17	4	1
24.75–25.00	35	22	13	3
>25.00	27	8	19	2

(Number of excess objects found on HCF = 19)

	APM	APM and HCF	APM and not HCF
22.00–22.50	6	6	0
22.50–23.00	10	10	0
23.00–23.50	16	10	6
23.50–24.00	26	20	6
24.00–24.50	29	28	1

Note: 1. Excess number found on HCF only = 70; 2. CCD frames of a subarea verified 1/9 of APM-only objects; 3. CCD frames verified 61/63 of the HCF-only objects.

2.3 Identification of faint clusters

The simplest criterion defining a candidate cluster is via an enhancement, above the mean background, in the surface density of galaxies within a specified area. The degree of contrast, σ_{cl}, can be defined via $\sigma_{cl}=(N_{cl}-N_f)/\sigma_f$, where N_{cl} is the number of galaxies in the area centred on the cluster to some chosen limit (in this case the visual limit of the HCF), N_f the mean background *field* count, and σ_f its variance, as determined from counts within similar areas randomly placed on that film.

Since the background count variation across an individual photographic plate may be greater than its Poissonian $\sqrt{N_f}$ value, σ_f can only be estimated by direct counting. Also the area within which N_{cl} and N_f are estimated is a crucial parameter in determining the nature and redshift range of the clusters sought. Since our goal is to find clusters that extend the redshift range of the Abell catalogue, we select a small area appropriate to a core diameter of ~ 1.5 Mpc for $H_0=50$ km s^{-1} Mpc^{-1} (Bahcall 1977; Couch *et al.* 1984) which, for $0.4<z<0.7$, corresponds to an angular diameter of 3.1 ± 0.3 arcmin or 12 ± 1 mm at the AAT prime focus.

The detection and classification of clusters proceeded as follows.

(i) Each 20×25 cm^2 HCF was divided into square sections of side 10 arcmin (about 40 mm) which serve as a grid for future reference. There are typically 25–30 such sections on each of the 55 plates.

(ii) On each film a circular aperture of diameter 3 arcmin was randomly placed $\simeq 12$ times and the number of objects lying within this aperture was recorded as an estimate of the local background. Obvious bright (<21 mag) stars were not counted, but no attempt was made to discriminate between faint galaxies and stars. Spectroscopic surveys (e.g. Colless *et al.* 1990) have confirmed that the proportion of stars fainter than $b_J\sim22$ is small (<20 per cent).

(iii) Each section was scanned by three independent observers (IM, WJC and RSE) and the locations of any apparent density enhancements of faint objects above the background was recorded. At this stage no account was taken of the degree of concentration or the brightness of the objects being examined.

(iv) The number of galaxies within a 1.5 arcmin radius of the centre of the enhancement was counted and, together with the background counts and its variance *for that particular film*, this gave the significance, σ_{cl}, of the enhancement.

(v) For those few fields with plates in both J and F, each was scanned independently and the catalogue merged later (see below).

The above criteria are simple and, in effect, follow reasonably closely those adopted by Abell in his Schmidt-based search, except, of course, he used original sky survey negatives. The major difference here is that no additional restriction relating to the number (richness) of galaxies contained within some magnitude interval (e.g. $m(n):m(n)+2$ mag) below the nth brightest member was made. Since the probability of encountering unrelated projected objects increases with redshift, such an additional criterion would not necessarily improve the reality of the clusters and would be complicated to model.

Our search radius is somewhat smaller, in metric terms, than used by Abell (0.75 Mpc, *cf.* 3 Mpc for $H_0=50$), but examination of a selection of representative Abell clusters shows the visibly conspicuous portions are contained within a radius of 0.25–0.5 Mpc. We tested for a possible concentration bias using the density profile data published by Couch & Newell (1984) and Butcher & Oemler (1978) for a range of clusters with $z<0.37$. Whilst a smaller fraction (35–40 per cent) of the population is contained within our aperture than in Abell's, the value is independent of cluster concentration.

In Section 2.2 we showed that eye searching HCFs is a reliable means of detecting faint images, but we must now test the reliability of this technique in identifying density enhancements above the mean local background. Does the high-contrast technique affect the visibility of galaxies uniformly on all scales? How homogeneous are the films from field to field and what is the approximate limiting depth surveyed?

Although the measuring machine tests described earlier reveal the overall depths of the visually produced HCF lists, to check homogeneity and photometric limits quantitatively, we must return to the measuring machine data. The first question posed above was addressed by scanning with COSMOS a typical high-latitude film (made from AAT plate F1652) and comparing contours of constant object surface density as determined by eye and by machine. In scanning the film, the COSMOS surface brightness threshold for image detection was selected empirically by Dr H. MacGillivray (Royal Observatory Edinburgh) so that the overall object surface densities were similar and merging problems/spurious images were minimized.

Using the COSMOS data, we counted the number of machine-detected objects in 1.5×1.5 arcmin^2 bins to map the background count variations. Whilst the gross background counts reveal no obvious *gradient* across the film, 10 discrete structures were found of significance $\geq3\sigma$ (using the procedure discussed above). Each of these was examined further and compared with the eye-produced catalogue.

Of the 10 candidate COSMOS 'clusters', four arise from the break up of images around bright stars in the field, three are due to similar difficulties around large spiral galaxies, and the remaining three match with the three cluster candidates found by eye (Table 2). This high degree of contamination by fake clusters underlines the difficulties of automated searches at faint limits. That the mean background count N_f and its variance σ_f agree closely between the COSMOS and eye-balled scans is probably not surprising given that the COSMOS threshold was adjusted to match these. However, what *is* reassuring is that the significances for the clusters

Table 2. COSMOS and HCF clusters on F1652.

Method	Cluster	σ_{cl}	$\overline{N_f}$	σ_{bg}
COSMOS	22CR	3.7	38	7.6
	20CR	6.4		
	16BR	3.2		
HCF(Eye)	22CR	4.2	41	6.8
	20CR	>4		
	16BR	3		

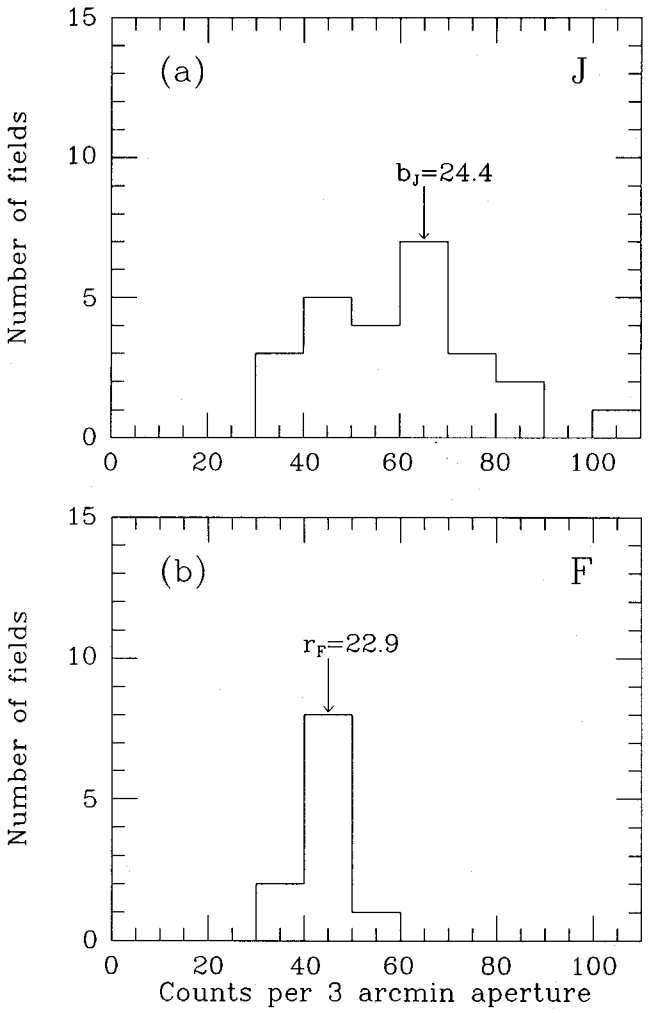

Figure 1. Distribution of the mean background source counts on each HCF film as determined from random sampling ≃12 areas per film. The median surface density for the *J* and *F* films is converted into an approximate limiting magnitude using published galaxy counts.

found by eye, σ_{cl}, agree closely with those measured objectively by COSMOS (Table 2).

We can address the second question: the approximate limiting magnitudes of the visual survey and the likely maximum variation from plate to plate, by comparing the surface density of galaxies N_f counted with those in published galaxy counts papers (*c.f.* review by Ellis 1988). The small contamination by stars at these limits (<5 per cent) is well within the uncertainties of the published counts. Fig. 1 shows the distribution of mean count (per 3-arcmin diameter circle) on each of the *J* and *F* films with the limiting magnitudes corresponding to the mode of the distribution marked. The most probable limiting magnitudes are $b_J = 24.4 \pm 0.3$, $r_F = 22.9 \pm 0.2$.

Given that a variation in surface density at a fixed apparent magnitude is seen even in *published* galaxy counts, clearly these are approximate values. Nonetheless, the limits above do agree with the limits obtained from an object-by-object comparison of those two plates, J1888 and J1836, studied in Section 2.2. There is a wider scatter in the *J* estimates than for *F*, in agreement with the study of Jones *et al.* (1991) who analysed the variation in CCD-calibrated COSMOS counts over somewhat larger areas (0.7 deg^2) across six AAT *J* plates and five *F* plates. The additional scatter in the HCF *J* films is unlikely to arise, therefore, from problems associated with applications of the high-contrast techique. Differences in galactic extinction and in viewing large-scale structures in the two pass-bands are explanations offered by Jones *et al.* The variance σ_f *on a given film* is largely Poissonian – i.e. there is no evidence for significant structures in two dimensions across a single prime focus plate.

Finally, we should note that the resulting catalogue of candidate clusters relies on agreement between the three observers *before* the significance is measured. The agreement between observers in terms of what was deemed worthy of further consideration is almost 100 per cent to about 2.0σ, and thus we adopted this as the working limit for the source catalogue. We demonstrate, however, in Section 3 below, that we can expect a small amount of contamination by spurious (unphysical) enhancements at the lowest σ values.

2.4 The catalogue

Table 3 lists the full catalogue of candidate clusters found from the 55 films of 51 fields to the cut-off $\sigma_{cl} = 2.0$. If a candidate cluster was found on films from *both J* and *F* plates for a given field, we merged the lists identifying the cluster with the pass-band showing the greater σ_{cl}.

The catalogue lists: (i) sequential plate number in the AAO archive; (ii) plate centre (1950); (iii) an internal grid reference identifying the cluster (of use only to the authors); and (iv) the value of σ_{cl} determined according to the procedures in Section 2.3. Accurate cluster positions are only available at this stage for a subset with $\sigma_{cl} > 4.0$ (see Section 4 and Table 3). The distribution of σ_{cl} values is shown in Fig. 2. A total of 112 clusters were found on 40 *J* films, as compared with 36 on 15 *F* films. In order to understand whether such a success rate on *J* and *F* films is to be expected, we attempt to model in Section 3 the anticipated distribution of clusters in our survey.

At this stage it is informative to consider the likely depth of the catalogue by comparing our candidates with published catalogues of brighter, nearby clusters found using Schmidt telescope material (Abell 1958; Abell, Corwin & Olowin 1989, hereafter ACO). Cross-correlating ACO's compilation (including their supplementary southern list) with our AAT fields, we find 17 ACO clusters lie in 13 of our 55 fields. Nine of the AAT fields were, in fact, purposely centred on an ACO cluster and therefore, although recognized in the scanning, were not catalogued since this would have unduly biased any statistical analysis. Of the remaining eight ACO clusters that lie by chance in the AAT survey, only one was catalogued by us. This is F1557.11BR(≡ACO3219) for which we have a spectroscopic redshift of $z = 0.151$ (Section 4); it is in fact the lowest-redshift cluster in our entire survey. Another likely low-redshift ACO cluster was missed (ACO3926), but retrospectively should perhaps have just satisfied our selection criteria, and the other six did not meet our criteria. It should be stressed that in no way should this be viewed as a criticism of our catalogue or the criteria, which are deliberately 'tuned' to finding clusters more distant

Table 3. Catalogue of clusters.

Plate	RA(1950)			Dec(1950)			Clusters	σ	z	Notes
J2172	00	35	00	-34	00	00	17C	6.0	0.348	
J1742	00	44	34	-21	01	08	18BL	7.0		
							9CL	3.8		
J1739	00	45	04	-25	34	11	5CB	2.8		
J1888	00	54	48	-27	54	46	16CL	5.3	0.563	1
							28CL	4.0		1
J1763	01	34	08	-13	10	20	14C	3.4		
							21CR	2.0		
J1566	02	00	02	-50	00	02	24TL	3.5		
							11C	3.2		1
							29BR	3.0		
							26TR	2.4		
							21TL	2.0		
J1779	02	44	18	-30	29	01	23TL	4.2		
							9BL	3.7	0.367	
							13BC	2.8		
							3CR	2.7		
							29CR	2.0		
J1780	03	20	30	-51	28	00	5BL	4.2	0.49:	3
							22CL	4.2		
							2TC	2.0		
J2073	03	26	18	-31	14	24	9/10C	4.3	0.275	
J2175	03	33	15	-39	10	02	15TR	5.1	0.41	
							23C	4.5	0.40	
							22C	3.6		
							29CR	2.2		
J1556	03	36	36	-35	38	07	15BL	5.6	0.457	
J1727	03	36	50	-26	32	51	23T	4.0		
							24TL	3.6		
							13C	3.2		
							30C	2.9		
J2059	03	41	41	-53	48	02	28TR	8.0		
J2183	03	44	45	-34	32	02	27TL	7.0	0.28:	3
							15CR	5.8		
							4TC	4.0		
							10TC	3.7		
							11BC	3.5		
J1765	03	53	46	-74	16	06	–	–		
J2000	04	00	30	-18	08	44	8LC	2.6		
J2089	04	14	56	-55	48	00	11TC	5.3		
							28BC	4.1		
							9TC	4.0		
							5TR	4.0		
							21TC	2.7		
							3C	2.3		
J1766	04	46	49	-20	49	56	10C	2.4		
							8BC/BR	2.0		
J2001	05	11	27	-48	27	47	21C	4.7	0.413	
J1772	05	11	39	-30	31	36	29TC	3.3		
							3BR	2.1		
J2077	09	21	16	-22	56	50	16C	2.2		
J1789	09	43	17	-14	05	50	–	–		
J2082	09	51	43	-27	03	04	–	–		
J2090	10	02	48	-07	28	01	7CL	9.1	0.378	
							9/10BC	4.2		
							3BR	3.1		
							4C	2.9		
J1816	10	39	12	-28	33	17	23BC	2.4		
							11C	2.3		
J1834	10	43	38	-00	04	49	5BC	4.6	0.442:	1,3
							8BL	4.4	0.445	
							3TC	4.1		1,4
							28BR	3.7	0.346	1
							2TC	2.8	0.377	1
							23CL	2.1		
							22C	2.0	0.469	1
							28C	2.0		
J1604	10	49	25	-09	04	04	10C	3.0		
J2091	11	10	54	-26	29	01	–	–		
J2026	11	48	30	-28	31	20	–	–		
J1614	12	00	41	-21	15	11	–	–		
J1872	12	19	26	-00	51	21	10C	2.9		
J2092	12	56	42	-14	45	58	17CL	3.5		
J1665	13	09	00	-01	06	00	–	–		
J2093	13	17	04	-26	46	08	23CL	5.3		
J2233	13	17	34	-00	00	30	10CL	3.0	0.424	
J1836	13	41	14	-00	00	30	3CR	7.7	0.414	1
							23TR	5.2	0.682:	1
							14RC	5.0	0.283	1
							10RC	4.6	0.275	1
J1824	13	41	14	-26	59	28	–	–		
J2094	15	04	00	+01	48	01	–	–		
J1884	20	48	13	-57	15	24	3TL	3.8	0.378	
J2056	23	21	46	-00	24	00	25/26	4.0		
F2262	00	54	48	-27	54	02	16CL	5.5	0.563	2
							28CL	2.5		2
F2057	02	00	00	-50	01	01	20C	4.6		2
							26TR	3.3		
F1557	04	08	58	-65	53	01	19TC	5.7	0.51	
							11BR	5.3	0.148	
							18BL	3.6		
							5C	2.9		
F1652	04	46	49	-20	49	57	20CR	> 4	0.412	
							22CR	4.2	0.48	
F1767	08	44	04	+18	03	50	10TC	7.0	0.664	
F1612	09	44	24	-08	34	15	22BC	3.5		
							22LC	2.3		
							27C	2.1		
F1835	10	43	38	-00	04	49	3TC	7.4		2,4
							2CL	5.4	0.377	2
							22CR	4.9	0.469	2
							28BR	4.6	0.346	2
							5BC	3.0	0.442:	2,3
F1613	12	00	41	-21	15	11	13C	2.5		
F2097	13	34	18	-29	36	58	–	–		
F1837	13	41	14	-00	00	30	23C	7.1	0.682	2
							3C	6.3	0.414	2
							15	3.8	0.283	2
							10C	3.2	0.275	2
							30BLX	2.5		
							28BR	2.2		
							11	2.0		
F2110	16	17	04	-15	31	14	–	–		
F1896	19	54	49	-32	33	49	–	–		
F1636	22	26	56	-21	02	37	28/29CT	4.1		
							14BR	3.5		
							11CR	3.1		
							24BR	2.5		
F1746	22	50	48	-33	58	04	24C	4.8		
							11C	3.6		
							9CT	2.0		
F1637	23	56	00	-32	39	40	23TL	5.2	0.48	
							23BC	5.1		

Notes: 1. Cluster also found on F plate; 2. Cluster also found on J plate; 3. Redshift based on one galaxy only; 4. Cluster found to be a projection effect (see text).

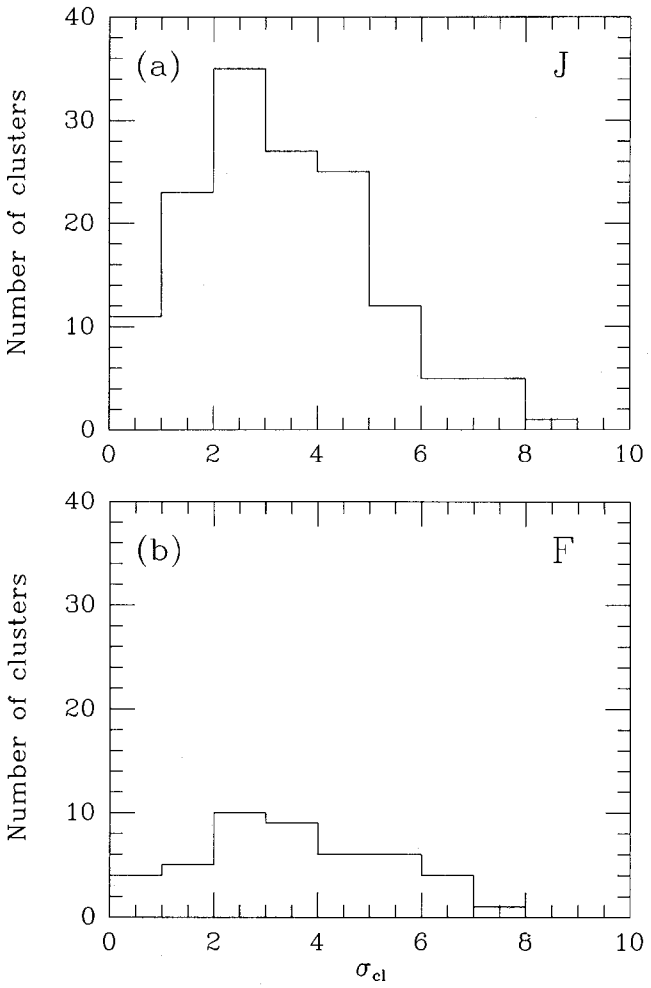

Figure 2. Distribution of contrast significance values σ_{cl} (see text for definition) for candidate clusters in the J and F surveys. Only those clusters with $\sigma_{cl} \geq 2$ are catalogued in Table 3.

than the ACO list. Of the six ACO clusters that fail to meet our criteria, four are simply too extended to produce significant contrasts within a 3 arcmin diameter circle and therefore are presumably at very low redshift (one occupies more than the entire AAT plate!), and two were very weak enhancements whose reality might be open to question.

3 MODELS

An important consideration in the construction of any catalogue is the extent to which the adopted selection procedures have excluded the sought-after objects while permitting the inclusion of those which are completely spurious. In this context the well-defined selection criteria for our catalogue discussed in Section 2.2, together with spectroscopic data we have accumulated (see Section 4) allows the questions of completeness and contamination to be scrutinized in some detail.

3.1 Simulations of the search procedure

As a means of assessing the completeness of our catalogue and possible effects of selection biases in our visual search technique, our search procedure was applied to a series of artificial 'fields' generated using a simple Monte Carlo 'hit–miss' technique to reproduce, as closely as possible, the apparent projected galaxy distribution encountered on our HCFs. The simulated ~ 1 deg^2 area of the HCF field was divided up into a grid of square cells equal in area to that of our 3 arcmin diameter aperture. A background 'field' galaxy population was created by distributing galaxies at random within each cell with the observed variation in number from cell to cell and the average count per field (Fig. 1).

'Clusters' were randomly superimposed in numbers (0–8) typical of those found on individual films; the exact number was selected at random from this range. The clusters were defined by three quantities: central concentration, redshift and contrast (as given by our σ_{cl} parameter). Central concentration was quantified via Butcher & Oemler's (1978) C index with each cluster being assigned a value drawn at random from the observed range for nearby clusters ($C = 0.3$–0.6; Butcher & Oemler 1978). Similarly a redshift was assigned to each cluster by randomly selecting from the observed redshift range for our clusters ($0.25 < z < 0.7$; Section 4). The contrast σ_{cl} was, on the other hand, preset for each cluster in a given field so that the success rate in a cluster detection could be monitored as a function of this parameter.

Since σ_{cl} is predefined, the number of cluster galaxies within a 1.5 arcmin radius of its centre is given by $N_{cl} = \sigma_{cl}\sigma_f + N_f$ (Section 2.3) regardless of the photometric selection function. The N_{cl} galaxies were distributed within a 1.5 arcmin radius according to a radial density profile appropriate to the assigned C index and redshift. For convenience we used the sequence of Aarseth model profiles published by Butcher & Oemler which provide excellent representations of the observed cluster profiles for a wide range of central concentrations.

For each artificial field, the computed galaxy distribution was viewed on a graphics display unit at a plate-scale identical to that of the HCFs with each galaxy being represented by a dot of 1.5 arcsec diameter ($\simeq$ the seeing on the plates surveyed); no attempt was made to incorporate photometric information at this stage. While this is an undoubted shortcoming, it is lessened by the HC process which enhances the visibility of the faintest objects whilst the brighter objects saturate. This has a compressive effect on the apparent magnitude range (see examples in Plate 1).

Three fields were simulated for each of 13 σ_{cl} values between 1.5 and 4.5 in steps of 0.25. Both 'J' and 'F' runs were conducted with the appropriate galaxy density (mean and variance). Each field was viewed 'blind' with respect to both the number of clusters it contained and its preset σ_{cl} value. This was accomplished by processing the fields in random order. Clusters were identified visually using exactly the same criteria as in our original search (see Section 2.3). Cluster locations were recorded and compared with the generated list to reveal both the number correctly identified and any 'false' clusters. In this context a 'false' cluster refers to a density enhancement in the background field distribution incorrectly identified as a cluster and not to systems at different redshifts overlapping along the line-of-sight. By simulating only the projected (rather than the three-dimensional) distribution of galaxies on the sky it was not possible to determine the likely occurrence of the latter type of systems.

The results of this experiment can be summarized as follows.

(i) Cluster identification was 100 per cent reliable in all fields where $\sigma_{cl} \geq 3.25$.

(ii) Below $\sigma_{cl} = 3.25$, cluster identification became increasingly incomplete. The first clusters to be missed are those of lowest central concentration ($C \sim 0.3$). At $\sigma_{cl} = 2.5$ the fraction of clusters successfully identified is < 10 per cent for the range $0.3 \leq C \leq 0.35$, 32 per cent for the range $0.35 \leq C \leq 0.45$ and ~ 70 per cent for $C > 0.45$.

(iii) This behaviour was observed for *both* the '*J*' and '*F*' runs despite the 50 per cent higher field densities and different σ_f values that apply in the *J* films. This suggests that the dominant factor in determining the visibility of a cluster is the *contrast* above the background as quantified by our σ_{cl} parameter.

(iv) A small number of 'false' clusters were identified in fields, but this population only became serious for $\sigma_{cl} < 2.0$. This result is consistent with the level at which there was discordance between the three observers in the inclusion of clusters in the actual catalogue (see Section 2.3).

One additional concern is that the presence of a central dominant galaxy (or galaxies) might preferentially attract attention to a cluster and hence increase the chances of its detection, especially in cases where the density contrast is low. Inspection of those clusters with $\sigma > 4$ suggests 14 ± 4 per cent are of Bautz-Morgan type I/I–II which is not significantly higher than Leir & van den Bergh's (1977) estimate of 7 per cent for the statistically complete Abell sample.

In summary, therefore, our simulations suggest that our catalogue of distant clusters should be complete in its identification for systems taxonomically similar to those found locally over a wide range in redshift down to a contrast level $\sigma_{cl} \simeq 3.25$, and that a significant number of concentrated (high C) clusters should be present at lower σ_{cl} values. Below $\sigma_{cl} \simeq 2.0$, serious contamination would be expected from spurious non-physical associations.

3.2 Predictions based on nearby cluster densities

The above estimate of completeness allows us to quantitatively address the questions of the numbers and type of clusters expected in our catalogue and their overall redshift distribution. We do this approximately since in Section 4 we report on a proper spectroscopic survey of a subset of the catalogue. The overall goal here is to provide an additional criterion on the reliability or otherwise of the catalogue in terms of the known distribution of Abell clusters (Abell 1958; ACO).

First we update the calculations of Couch *et al.* (1984), where the contrast, σ_{cl}, of an Abell richness class 3 cluster was determined in a number of pass-bands as a function of its redshift and evolutionary history, by extending the analysis to include other Abell richness classes (0, 1, 2 and 4) and, when appropriate, taking into consideration more up-to-date estimates of the evolutionary correction.

First, we consider the no-evolution case based on the b_J and r_F cluster luminosity functions published by Couch & Newell (1984) for Abell 1942, a richness class 3 cluster at $z = 0.22$ with an intermediate central concentration of $C = 0.45$. This cluster was chosen since it has *no* blue galaxy excess (Couch 1981). Field galaxy counts are taken from Peterson *et al.* (1979) and Koo (1981) with *K* terms from King & Ellis (1985). Luminosity functions appropriate to the other richness classes were derived by scaling those of the Abell 1942 cluster according to the median galaxy population between m_3 and $m_3 + 2$ upon which Abell defined each class. No corrections for environmental density effects were made.

The computed (σ_{cl}, z) relations are shown in Fig. 3. In the absence of any evolution our survey should be sensitive to Abell clusters at redshifts well beyond the limits of the Abell (or ACO) catalogue. The richness class 4 systems, for example, drop below our $\sigma_{cl} = 3.25$ completeness limit at $z = 0.75$ (F) and $z = 0.55$ (J). Even the poorest, class 0 systems, which Abell did not include in his statistically complete sample, should be detectable out to $z \sim 0.3$–0.4.

In predicting the *number* of clusters expected in any survey, an important factor is the frequency per comoving unit volume for clusters of different richnesses. We note, for example, that richness class 4 clusters make up a very small fraction of the Abell catalogue; their volume density may be too low for a significant number to be found in our survey. To approach this question we have estimated the comoving volume densities for each of the richness classes on the basis of the number of clusters Abell observed in each class. Here we use Abell's statistical sample (richness classes 1–4 only) which covered 41253 deg^2 of sky and which we assume is complete to $z \sim 0.2$ (Chincarini 1988). The resulting volume densities are summarized in Table 4 together with the (comoving) volumes sampled, and also the numbers expected in the AAT survey.

Table 4. Predicted numbers of Abell-type clusters.

Richness Class	ρ_{Abell} gal Mpc^{-3}	*J* Vol (Mpc^3)	N_{pred}	*F* Vol (Mpc^3)	N_{pred}
1	1.79×10^{-7}	5.16×10^{7}	9	8.06×10^{7}	14
2	5.61×10^{-8}	1.01×10^{8}	6	1.59×10^{8}	9
3	9.96×10^{-9}	1.73×10^{8}	2	2.20×10^{8}	2
4	8.79×10^{-10}	2.30×10^{8}	0	2.70×10^{8}	0

Note: $H_0 = 50$ km s^{-1}, $q_0 = 0.1$.

In calculating the sample volumes for each richness class, the high-redshift limit was taken to be that at which $\sigma_{cl} = 3.25$ (Fig. 3) on the assumption of no luminosity evolution. For a lower limit we used $z = 0.25$, the redshift below which our catalogue will almost certainly be incomplete because such systems will be substantially larger than our 3 arcmin diameter sampling area. The remaining quantity required to make this calculation, the solid angles covered by our search, was 36 and 13.5 deg^2 for the blue and red plates, respectively.

The predicted cluster statistics are not unduly sensitive to the parameters defining the depth of our survey. A shallower plate limit reduces the visibility of both cluster and field galaxies alike and thus the resulting change in σ_{cl} must be carefully computed. A reduction, for example, on the effective limiting *J* magnitude of 0.3 mag (the scatter in Fig.

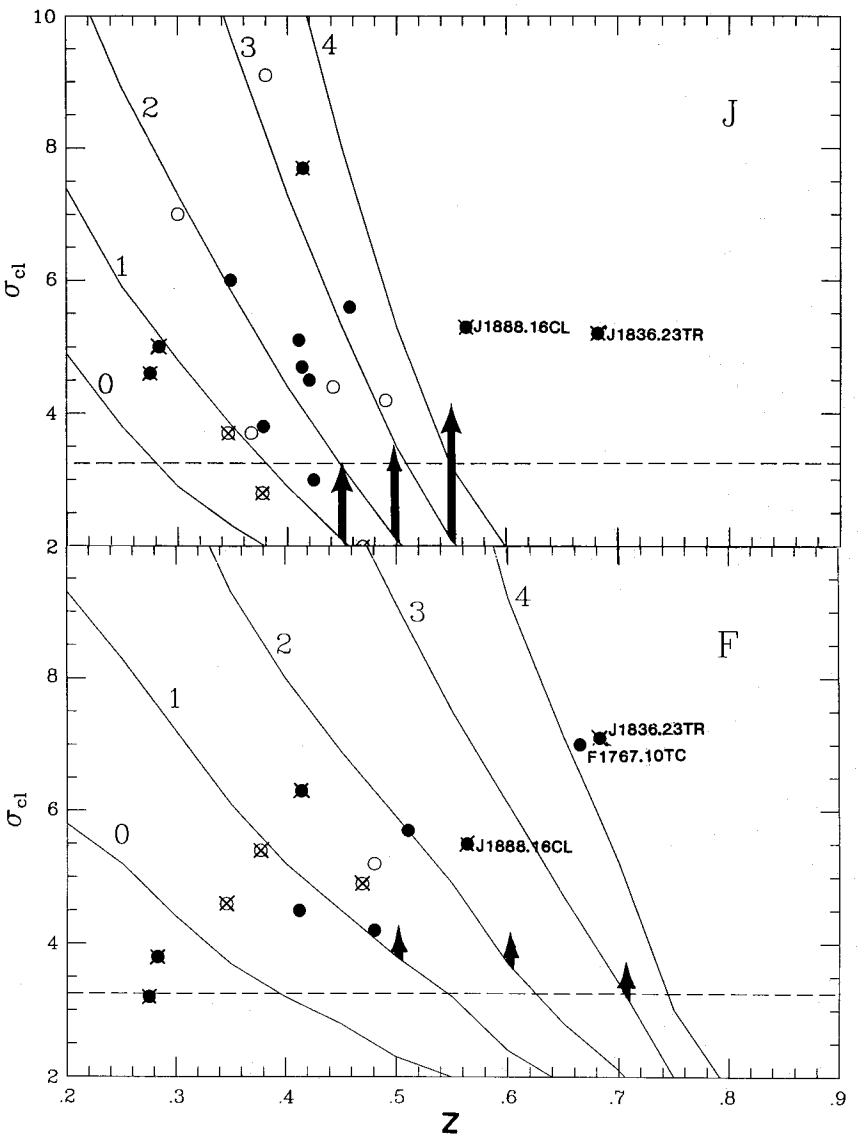

Figure 3. Computed contrast significance $\sigma_{cl}(z)$ relations for clusters of various Abell richness classes (0–4) in the absence of luminosity or clustering evolution for samples selected in *J* and *F*. Spectroscopically confirmed clusters from the survey are plotted. Open circles denote clusters whose redshifts remain slightly uncertain. Crossed circles denote clusters detected in both colours. The dotted line represents the completeness limit of the catalogue (Section 3.1). Arrows indicate the effect a short-term burst of star formation for a subset of the cluster population would have on its visibility (see Section 5.3 for details).

1) increases the σ_{cl} completeness limit from 3.25 to 3.6. A limit *deeper* by the same margin lowers the completeness to $\sigma_{cl} = 2.9$. Since these completeness values vary fairly symmetrically about the means adopted, and the $N(\sigma_{cl})$ relation is fairly flat above the completeness limit (Fig. 2), we estimate the uncertainty introduced in the predicted number of Abell clusters by variations in the homogeneity of our survey should be smaller than $\simeq 10$ per cent.

We see in Table 4 that the richness class 1 clusters should be the most common in our samples of both colours. The number of clusters in the higher-richness classes is predicted to decrease monotonically with increasing class number. As we suspected earlier, richness class 4 systems occur so rarely that none are expected to appear within our catalogue.

It is interesting now to compare the *total* number of clusters predicted with that actually detected. Adopting our completeness limit of $\sigma_{cl} = 3.25$, a total of 23 *F* cluster candidates were found compared to a no-evolution prediction of 25. This contrasts with the 44 *J* clusters above the same σ_{cl} limit, which is much larger than the expected number of only 17.

Thus the detection rate for *F* and *J* clusters per unit area is fairly comparable (see Section 2.4) yet our model predicts there should be a far lower *J* success rate than is actually observed. Whilst the modelling is subject to some uncertainty, there are nevertheless good physical reasons for understanding at least some enhancement in the surface density of *F* clusters. One factor is the energy distribution of the early-type galaxies which form the bulk of the galaxy population in the cores of rich concentrated clusters. At the mean redshift of the survey, $\bar{z} \simeq 0.45$ (see Section 4) the *K* corrections at *F* and *J* differ by 0.4 mag which progressively

dims early-type galaxies in J, making faint clusters disappear more readily and at lower redshifts.

That the actual number of J clusters is $\simeq 2$ times that expected is therefore an important result. A number of possibilities arise.

(i) *Evolution.* Our predictions are based on the non-evolution case; if early-type members were brighter and bluer in the past then the predictions will underestimate the number of clusters expected (both via luminosity and depth effects). The major challenge to this explanation is whether any form of evolutionary brightening can conspire to produce such a significant enhancement of numbers in our J band while at the same time having little or no effect in our F band.

(ii) *Overlapping clusters.* Many clusters may have had their contrast enhanced through projected overlaps with other systems along the line-of-sight. If the contaminants are predominantly weak foreground systems with a great proportion of blue spirals, then the incidence of cataloguing such systems would be higher in the J band.

(iii) *Weak nearby clusters.* Rather than finding clusters at high redshift dominated by early-type galaxies, our search may have picked up a large number of very poor systems (richness class 0 or less) that are relatively nearby ($z < 0.2$) and which contain a higher fraction of spirals. Our model predictions cut-off at richness class 0 and it is possible that the excess J sample is made up of weaker systems.

We will return to these hypotheses after reporting on the second stage of our survey – namely, the spectroscopic observations of a complete subset of the catalogue.

4 SPECTROSCOPIC SURVEY

Our original plan for the second stage of the survey was to follow up each of the candidates in Table 3 with deeper broad-band CCD images to provide photometric information, both to better quantify the contrast and reality of the clusters and to select targets (by colour) for spectroscopy. Such a strategy was adopted by GHO.

We modified this plan for two reasons. First, simulations (Couch *et al.* 1984 and Section 3) revealed that a gain of $\sim$ 0.5 mag (such as would be possible with a ~ 500 s R/I exposure with a CCD) would not significantly improve the contrast. In particular, deeper images would not help distinguish which clusters were genuine and which were overlapping groups at diverse redshifts, which we rightly perceived as the main difficulty at these faint limits. Secondly, at that time, we did not have access to an instrument with an imaging and spectroscopic capability. Thus, imaging all the candidates in Table 3 would consume many nights of telescope time and would not obviate the need for further spectroscopic-time requests. The HCFs already penetrate deep enough to provide an adequate target list, and consequently we decided to proceed directly to a spectroscopic follow-up programme.

The spectroscopic survey was essential not only to determine the redshift of each cluster but also to test the degree of contamination from intervening field galaxies. Such a survey has additionally the benefit of checking the three hypotheses presented in Section 3.2 for the excess number of blue clusters. In the case of Abell's catalogue, Lucey (1983) predicted that as many as ~ 20 per cent of the clusters in the sample are structures without physical significance arising from projection effects. The chances of this occurring in our much deeper catalogue are likely to be greater.

Spectra of our cluster galaxies have been obtained over 5 years (1985–90) on a number of large telescopes using a variety of instruments. Ideally, we would have liked to have obtained spectra for all 58 clusters whose σ_{cl} exceeded the completeness limit of the catalogue (> 3.25). Unfortunately, the short supply of large-telescope time and the time-consuming nature of the observations restricted the sample we could realistically observe. Instead, we embarked on spectroscopy for only those 44 clusters with $\sigma_{cl} > 4.0$. By selecting a σ-limited subset we should still be able to understand the resulting redshift distribution in terms of the models discussed in Section 3. For example, in the non-evolving case (Fig. 3), this rise in the σ_{cl} cut-off corresponds to a reduction of only $\Delta z \simeq 0.05$ in the maximum depth of the survey.

The vagaries of weather meant that even this sample was not completed. Of the 44 clusters, satisfactory spectra were only obtained for galaxies in 28. A major limitation was our rule, nearly always maintained, that a cluster redshift was only completed when more than one galaxy was observed with the same redshift. However, by aiming to complete individual fields to our σ_{cl} limit wherever possible, we have managed to maintain a complete sample. Rather than completing the spectroscopic survey of all 51 AAT fields to $\sigma_{cl} > 4.0$, we have in effect completed a subset of 11 fields to this σ_{cl} limit and have incomplete data on a further six fields. Whilst the sample is small, we are nevertheless in a position to place some constraints on the models developed in Section 3.

Finding charts for those clusters for which spectroscopy has been obtained are shown in Plate 1. We have chosen to present the original HCF pictures even for those few clusters for which CCD images are available. This provides a uniform set of material from which targets were selected; those galaxies for which successful spectra were obtained are marked on the charts. A summary of the details relevant to the redshift observations is given in Table 5. We include the telescopes and associated instrumentation used (columns 1

Table 5. Summary of redshift observations.

Telescope	Instrument	Dispersion (Å mm^{-1})	Resolution (Å)	Wavelength Range (Å)	Dates
(1)	(2)	(3)	(4)	(5)	(6)
AAT 3.9m	FORS	450	15–20	5200–11000	Mar 1985 Dec 1985
AAT 3.9m	LDSS	164	9	3500–7500	Oct 1986 Mar 1987
ESO 3.6m	EFOSC	230/270	13/14	3600–7000/ 5600–9900	Sept 1986 Nov 1987
WHT 4.2m	FOS–2	400	14	4600–9700	Oct 1987 Dec 1987 Feb 1988 Jun 1988 Jan 1989 Feb 1990
INT 2.5m	FOS–1	486	15–20	5000–10000	Dec 1984

and 2), the dispersion and resulting resolution (columns 3 and 4), the wavelength range (column 5), and the dates when the observations were made.

Table 6 summarizes the spectroscopic results. We include redshift data both for members and interlopers, and those few objects which turned out to be stars. At an early stage in the project, spectroscopy was obtained for one cluster (J1884.3TL) with $\sigma_{cl} < 4.0$. We include this result in the spectroscopic catalogue, but do not use it in the subsequent analysis.

For the spectroscopic work we used a variety of high-throughput spectrographs optimized for faint-object work. Briefly, the Faint Object Red Spectrograph (FORS) on the 3.9-m AAT and the Faint Object Spectrographs (FOS-1, FOS-2) on the 2.5-m Isaac Newton (INT) and 4.2-m William Herschel Telescopes (WHT), respectively, are similar, collimatorless, fixed-format devices with a single, low-dispersion grism blazed at ~7500 Å and a red-sensitive 385×576 22 μm pixel GEC CCD as detector. Detailed descriptions of the FOS-1 and FOS-2 can be found in Breare *et al.* (1987) and Allington-Smith *et al.* (1988), respectively.

The Low Dispersion Survey Spectrograph (LDSS) at the AAT and the ESO Faint Object Spectrograph and Camera (EFOSC) on the ESO 3.6 m are somewhat more versatile instruments which achieve much the same high throughput as the FOS design despite having collimation optics. As focal-reducing imagers they have facilities for multi-object slit spectroscopy (Ellis & Parry 1988). Both offer a wider choice of grisms allowing us to work at a slightly higher dispersion than with the other systems with obvious advantages for the detection of weak absorption lines. Both were used with RCA CCDs of the low-noise ($\sigma_{read} \sim 35 e^-$) SID 501 EX variety.

The faintness of the cluster galaxies ($R \sim 18$–22) demanded high-precision astrometry. Positions to ~ ±0.3-arcsec rms accuracy were determined for a wide selection of candidate galaxies and bright stars in each cluster field by first establishing a secondary sequence of astrometric standard stars on the AAT plate using appropriate Palomar or UK Schmidt plates, and then completing a secondary set of measurements on the HCF itself. Measurements were made using the AAO PDS microdensitometer or the Packman XY-measuring machine at the Royal Observatory Edinburgh. The positions of most galaxies for which spectroscopy was obtained are included in Table 6.

The observing strategy used to determine the redshift of the cluster was to obtain a minimum of two galaxies with the same redshift. In 75 per cent of the clusters this was

Table 6. Cluster galaxy redshifts.

Cluster	Object	RA(1950)	Dec(1950)	z	Instrument[1]	Comments
J2172.17C	a	00 35 02.0	-34 09 47	0.348	E	
	c	00 35 01.3	-34 09 56	0.348	E	
J1888.16CL	1	00 54 31.5	-27 56 44	0.561	E	
	5	00 54 30.4	-27 56 38	0.566	E	
J1779.9BL	3	02 43 19.1	-30 34 54	0.365	E	
	4	02 43 21.3	-30 34 39	0.37	E	
	2	02 43 22.3	-30 35 01	0.53	E	
	9	02 43 23.1	-30 35 20	0.33:	E	
	y	-	-	0.30	E	
J1780.5BL	a	03 21 43.4	-51 16 00	0.49	E	
J2073.9/10C	a	03 25 52.1	-31 13 55	0.275	W	
	b	03 25 50.9	-31 13 50	0.275	W	
J2175.23C	a	03 31 08.0	-39 16 49	0.40	E	
	b	03 31 08.5	-39 16 56	0.40	E	
	c	03 31 08.9	-39 17 02	0.40	E	
J2175.15TR	a	03 32 29.7	-39 03 58	0.41	E	
	d	03 32 29.4	-39 04 03	0.41:	E	
	j	03 32 30.4	-39 03 42	0.41	E	
J1556.15BL	2	03 37 31.0	-35 38 56	0.457	F	
	2	03 37 31.0	-35 38 56	0.456	EM	
	8	03 37 31.0	-35 39 17	0.457	F	
	10	03 37 32.6	-35 39 01	0.466:	EM	
J2183.27TL	a	03 45 36.7	-34 46 46	0.28	E	
	b	03 45 35.5	-34 46 42	0.0	E	star
F1557.11BR	a	04 05 39.7	-65 43 58	0.151	F	
	b	04 05 38.2	-65 43 44	0.145:	F	
F1557.19TC	a+b	04 12 34.4	-65 58 30	0.51	E	
	c	04 12 33.6	-65 58 17	0.51	E	
F1652.20CR	1	04 45 52.4	-20 42 50	0.414	W	
	2	04 45 52.1	-20 42 41	0.41	W	
	3	04 45 52.6	-20 42 33	0.0	W	star
F1652.22CR	1	04 47 12.3	-20 38 48	0.48	W	
	2	04 47 13.5	-20 39 27	0.44:	W	
	3	04 47 13.4	-20 39 03	0.48:	W	
	4	04 47 15.7	-20 38 45	0.0	W	star
J2001.21C	1	05 12 14.4	-48 21 54	0.406	F	
	1	05 12 14.4	-48 21 54	0.42	E	
	5	05 12 17.1	-48 21 47	0.414	F	
	x	-	-	0.411:	F	
	3	05 12 18.6	-48 21 50	0.11	E	
F1767.10TC	g	08 44 52.0	18 04 37	0.665	F	
	j	08 44 56.9	18 05 07	0.438	F	
	y	08 44 53.6	18 05 02	0.0	F	star
	c	08 44 52.7	18 03 34	0.653	L	
	d	08 44 53.4	18 04 03	0.663	W	
	a	08 44 52.2	18 03 53	0.562:	W	
	s	08 44 55.9	18 04 28	0.0	W	star
	e	08 44 51.7	18 04 22	0.673:	L	
J2090.7CL	a	10 02 12.8	-07 06 17	0.376	W	
	α	-	-	0.38	W	
J1834.3TC	a	10 42 06.3	00 01 20	0.150	F	
	f	10 42 06.7	00 01 46	0.274	F	
	m	10 42 03.7	00 01 20	0.560	F	
	y	-	-	0.231	F	
J1834.5BC	a	10 42 37.4	-00 14 50	0.442	W	
J1834.8BL	a	10 43 18.6	00 17 31	0.442	W	
	b	10 43 18.5	00 17 33	0.448	W	
F1835.2CL	a	10 42 11.2	00 15 12	0.375	F	
	b	10 42 11.3	00 15 08	0.500	F	
	u	-	-	0.379	F	
F1835.22CR	a	10 44 28.4	-00 11 17	0.474	F	
	b	10 44 28.4	-00 11 22	0.465:	F	
	d	10 44 28.5	-00 11 40	0.000	F	M star
	x	-	-	0.576	F	
	y	-	-	0.229	F	
F1835.28BR	a	10 45 04.1	-00 07 31	0.346	F	
	b	10 45 03.8	-00 07 29	0.346	F	
J2233.10CL	c	13 16 53.1	-21 33 27	0.424	F	
	g	13 16 52.7	-21 33 03	0.424	F	
J1836.23T	a	13 40 32.4	00 14 00	0.400	F	
	e	13 40 34.0	00 13 26	0.685	F	
	p	13 40 33.4	00 13 40	0.587:	F	
	x	-	-	0.417	F	
	22	13 40 33.6	00 12 19	0.436	LM	
	g	13 40 33.6	00 13 04	0.501:	LM	
	18	13 40 31.5	00 14 05	0.000	LM	star
	53	13 40 28.2	00 14 33	0.714:	LM	
	93	13 40 30.9	00 15 17	0.679	LM	
J1836.14RC	a	13 41 10.6	-00 15 46	0.283	F	
	l	13 41 10.7	-00 15 26	0.283	F	
	x	13 41 08.0	-00 16 31	0.283	W	
	z	-	-	0.284	F	
	u	-	-	0.583	F	
J1836.10RC	a	13 41 44.2	00 04 45	0.275	I	
	b	13 41 43.6	00 04 46	0.275	I	
J1836.3CR	a	13 42 28.1	-00 05 51	0.415	F	
	n	13 42 27.2	-00 05 47	0.417	F	
	d	13 42 28.3	-00 05 53	0.412:	F	
	k	13 42 26.8	-00 05 44	0.319:	F	
J1884.3TL	1	20 45 39.3	-57 06 24	0.374	E	
	3	20 45 37.4	-57 06 32	0.378	E	
	4	20 45 38.3	-57 06 19	0.381	E	
F1637.23TL	1	23 56 42.5	-32 34 02	0.48	E	
	4	23 56 41.3	-32 33 55	0.48	E	
	5	23 56 43.3	-32 34 06	0.48	E	

[1]E = EFOSC (long-slit), EM = EFOSC (multi-object mode), F = FORS, W = FOS on WHT, I = FOS on INT, L = LDSS (long-slit), LM = LDSS (multi-object mode).

1991MNRAS.249..606C

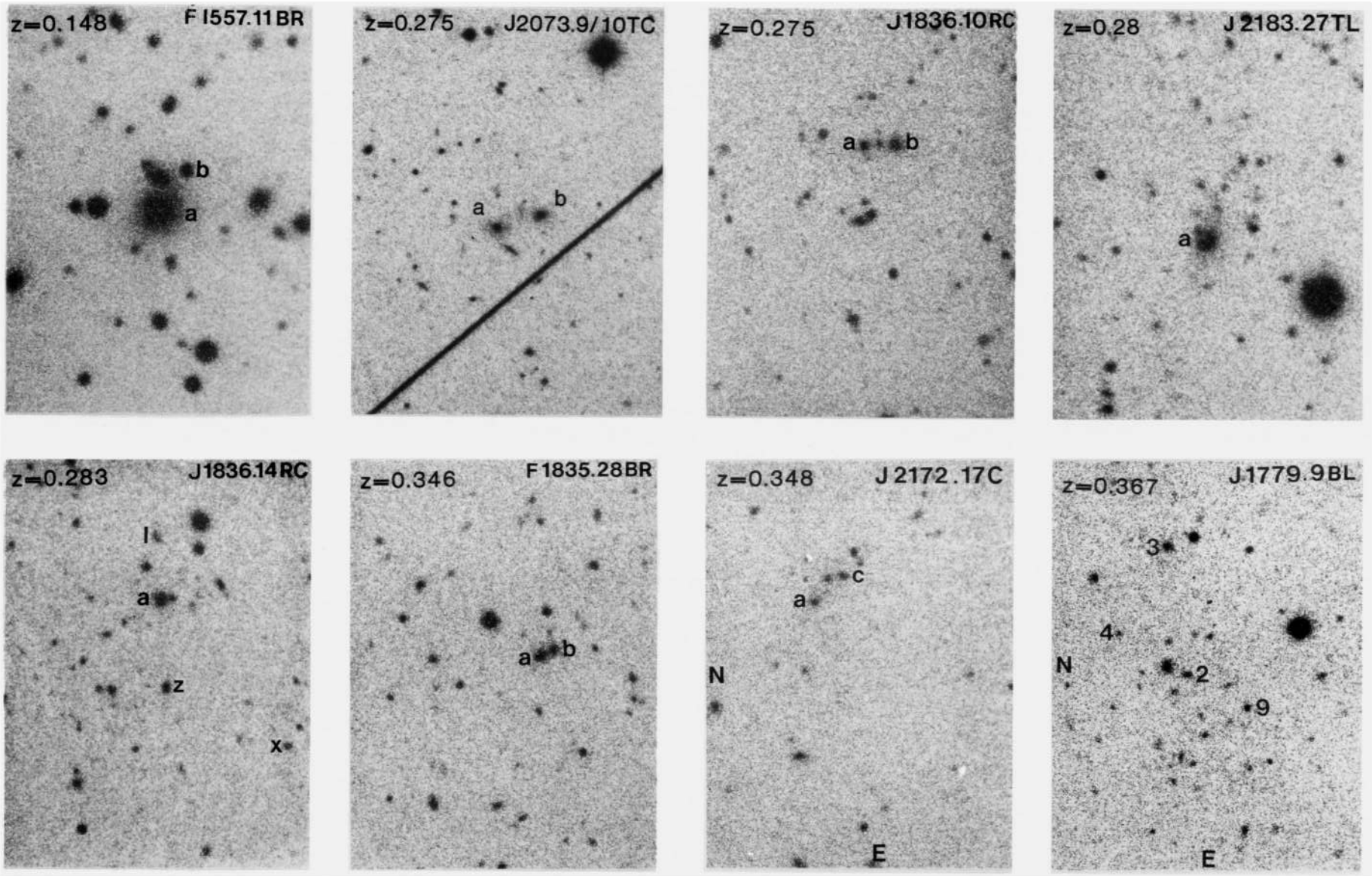

Plate 1. Finders for the clusters with spectroscopic redshifts in order of increasing redshift. North is at the top, east is to the left (unless otherwise marked) and each finder is 9.8×13.1 arcmin. The cluster and redshift are indicated and marked galaxies are those with spectroscopic identifications (see Table 6).

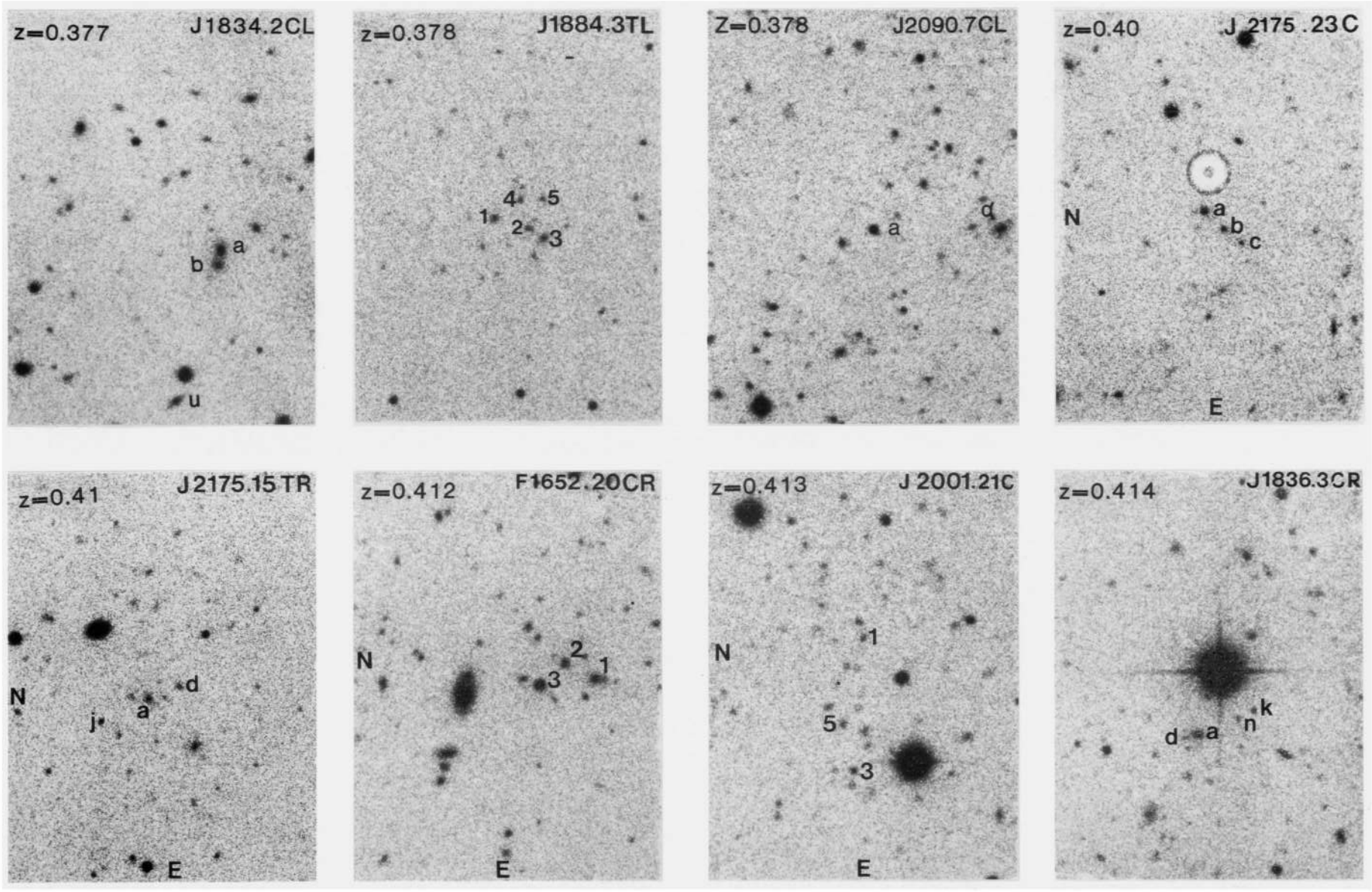

Plate 1 – *continued.*

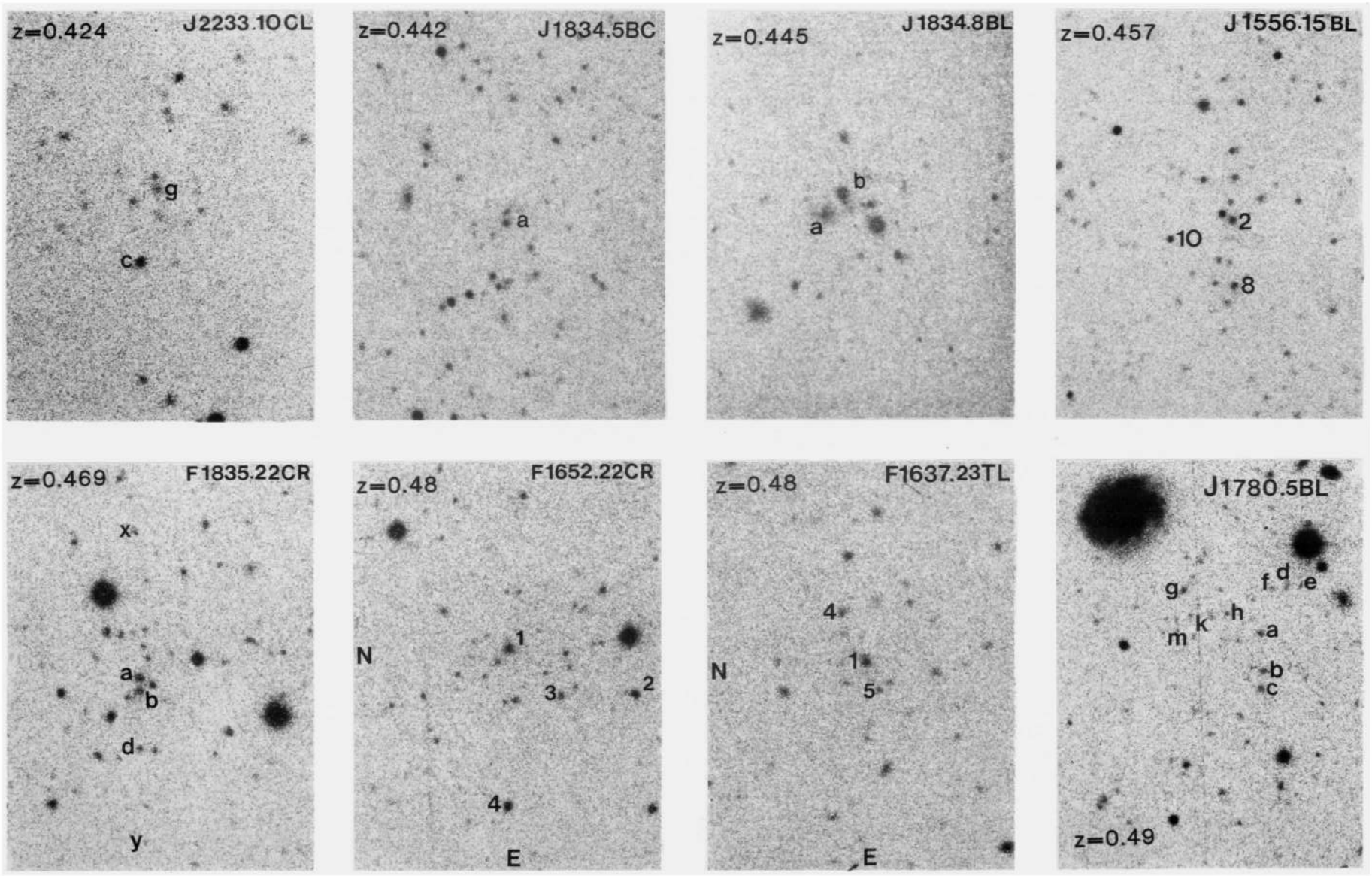

Plate 1 – *continued.*

1991MNRAS.249..606C

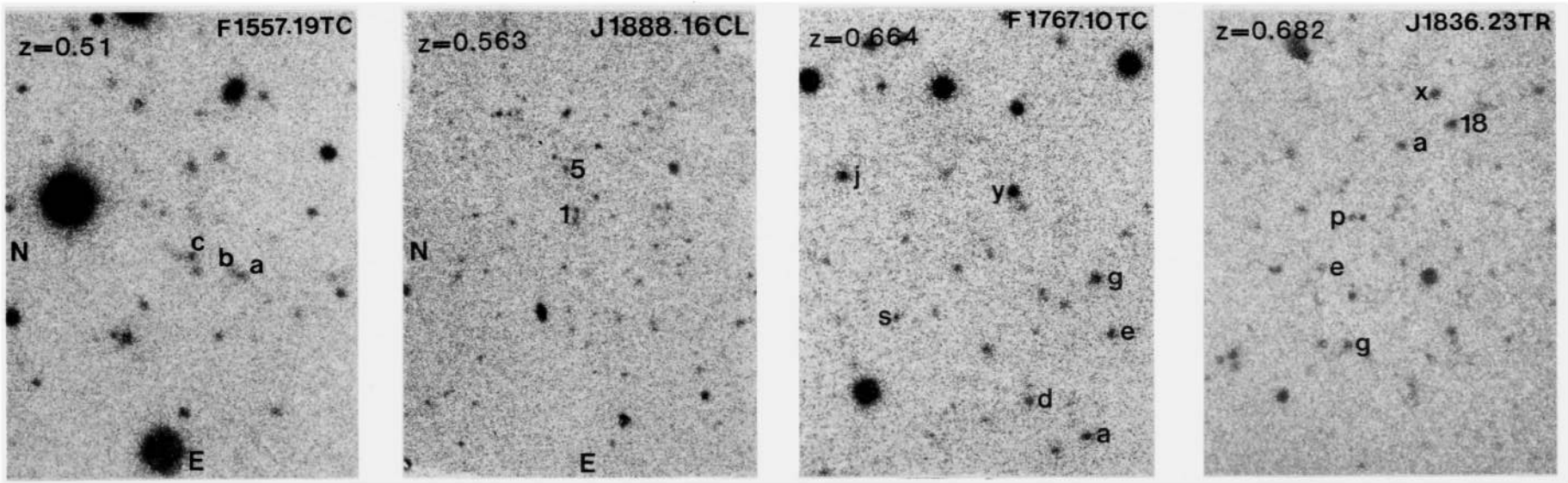

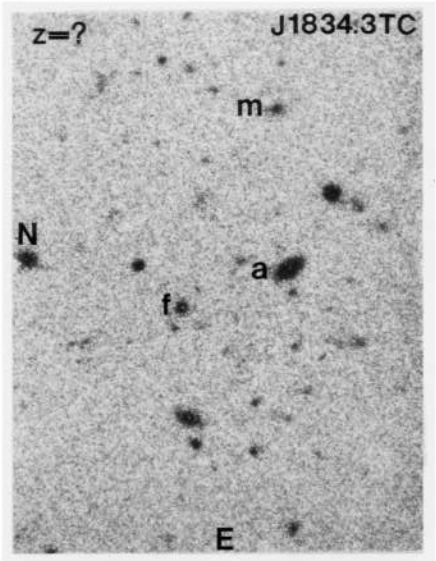

Plate 1 – *continued.*

achieved. For this reason the majority of our redshift observations were done in long-slit mode. Often three galaxies could be aligned on a long slit. If no matching pair of redshifts was found, additional long-slit exposures were taken on other promising candidates. For two of our clusters multi-slit exposures were taken using pre-prepared aperture masks. However, successful though these techniques have been for clusters *known to be of interest*, the overheads in acquisition and the added preparatory work make this a prohibitive strategy for simply determining the cluster redshifts.

Integration times varied but were generally in the range 3000–8000 s divided into intervals of 1000–2000 s to keep contamination of the CCD frames from cosmic ray events to a tolerable level and to simplify their removal during data reduction. Since preliminary 'on-line' reduction of a spectrum was possible within a few minutes at all telescopes, shorter exposures enabled efficient monitoring of progress and determination of the optimum exposure time. For the observations with FORS and FOS, the slit width was kept to 1.5–2.0 arcsec, irrespective of the seeing, in order not to compromise the already low intrinsic resolution of these spectrographs. For EFOSC and LDSS we chose 1.5 and 1.7 arcsec widths, respectively, to match the seeing at the time of those observations. At these slit widths our programme galaxies have slit magnitudes in the range $R_{\rm slit} \sim 19.5$–23.0.

Spectra were extracted and sky-subtracted using software developed by I. R. Parry for the INT FOS, but modified here for more general use. The spatial extent of each object and the areas from which the sky spectrum is sampled is determined interactively. Sky subtraction is performed by carefully determining the sky spectrum *underneath* the object by parabolic interpolation between broad bands of uncontaminated sky on either side of the object with automatic rejection of cosmic rays. Coaddition of individual spectra was done according to the weighting scheme of Robertson (1986).

A representative sample of spectra are shown in Fig. 4. Most of the galaxies sampled are representative early-type members with familiar absorption lines and continuum breaks. This is not surprising given we generally observed the cluster core, invariably aligning two or more prominent central galaxies. Occasionally the slit intersected a peripheral emission-line member, but the number of strong-lined objects, even interlopers, is considerably less than found using spectroscopy of similar resolution in the field (*cf.* Colless *et al.* 1990 and Section 5).

The spectra are not of sufficiently high quality to warrant a cross-correlation analysis or more detailed line analyses (e.g. incidence of Balmer features). Redshifts were measured manually by using a graphics terminal, deriving a redshift for each feature and taking the mean. Redshifts which are based on only a single line identification are indicated by a colon in Table 6.

Cluster redshifts have been derived by taking a mean of the values obtained for the galaxies observed in each case, after excluding obvious foreground and background objects; the latter procedure is not critical. The individual redshifts are given in column 5 of Table 6, with the cluster means listed in column 6 of Table 3. In cases where only one galaxy has been observed in a cluster field, we quote its redshift in Table 3 with a colon. One cluster (J1834.3TC) has four galaxies with different redshifts and may therefore be a spurious cluster.

In total, spectra were obtained for 95 galaxies in 29 clusters, a mean of 3.3 objects per cluster. Of the 95 galaxies, 66 are members (a mean of 2.3 members per cluster). Although a $\sigma_{\rm cl} > 4.0$ cluster should provide a field galaxy-to-cluster galaxy ratio of 2:1 over a 3-arcmin diameter, we have probably been fortunate in selecting the right targets as members because the contrast increases in the core where the targets were usually chosen.

5 DISCUSSION

5.1 The redshift distribution for a complete sample of clusters

As discussed in Section 4 it has not been possible with the telescope time available to complete the spectroscopy for a $\sigma_{\rm cl}$-limited sample in all 51 AAT fields. However, to the adopted limit $\sigma_{\rm cl} > 4.0$, redshifts have been obtained for all clusters found in 16 fields. This includes, of course, the five fields where no such clusters appear, and it allows us to determine the true surface density of $\sigma_{\rm cl} \geq 4.0$ clusters for a complete sample. We do this for both *J*- and *F*-selected samples and present the resulting cluster redshift distributions $N(z)$ alongside those for the $\sigma_{\rm cl} > 4.0$ sample of Table 6 in Fig. 5.

In Section 3 we demonstrated that a no-evolution prediction matches the observed number of clusters to $\sigma_{\rm cl} = 3.25$ but fails to produce the expected number of *J* clusters. A recomputation of the predictions for $\sigma_{\rm cl} > 4$ reveals the same conclusion. The number predicted in *F* is 16 (*cf.* 17 found) and there is an excess in *J* with 12 clusters expected compared to 26 found.

Fig. 5 also shows, from our simulations, the expected redshift distribution in the absence of any evolutionary effects or contamination problems. Although the redshift data reveal a marked paucity of systems with $z < 0.2$ (the nearest *J* cluster has $z = 0.28$ while the *F* sample has one cluster at $z = 0.15$ and the next at $z = 0.28$), this is largely because of our search diameter of 3 arcmin. The obvious selection against local clusters is, of course, allowed for in the model predictions.

The broad agreement between the range of cluster redshifts observed and predicted, i.e. the paucity of observed clusters with $z < 0.2$, allows us to reject hypothesis (iii) in Section 3.4 – namely that the excess of *J* clusters arises from the inclusion of a large number of feeble, low-redshift, blue groups. However, that the mean redshift of the complete *J* sample is similar to that of the *F* sample is surprising. The *F* redshift distribution matches the predicted curve reasonably well, but a surprising number of *J* clusters are at high redshift. We return to possible explanations for this result in Section 5.3.

5.2 Comparison with the sample of Gunn, Hoessel & Oke

Gunn *et al.* (1986) have catalogued a similar *northern* sample of distant clusters, many of which have spectroscopic measurements. These authors used a variety of source material, including Mayall 4 m *F* and *N* (700–850 nm) prime focus plates totalling a survey area of 29.4 deg^2 and Hale 5 m

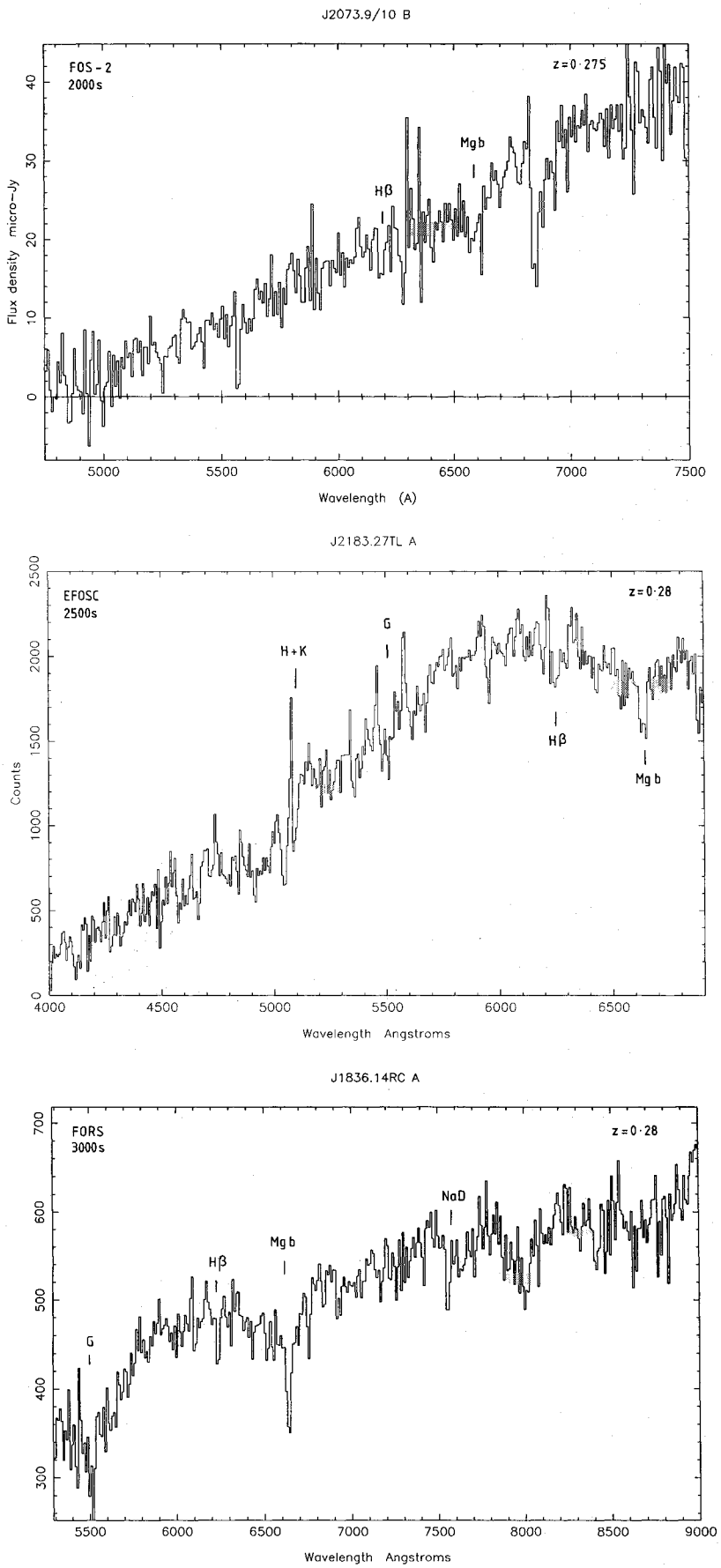

Figure 4. Representative results from the spectroscopic survey with target, instrument, exposure time, features and redshift marked.

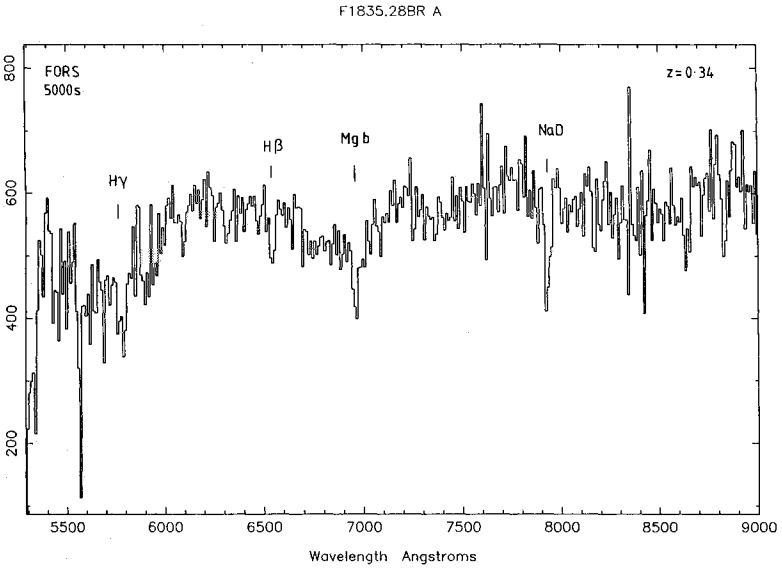

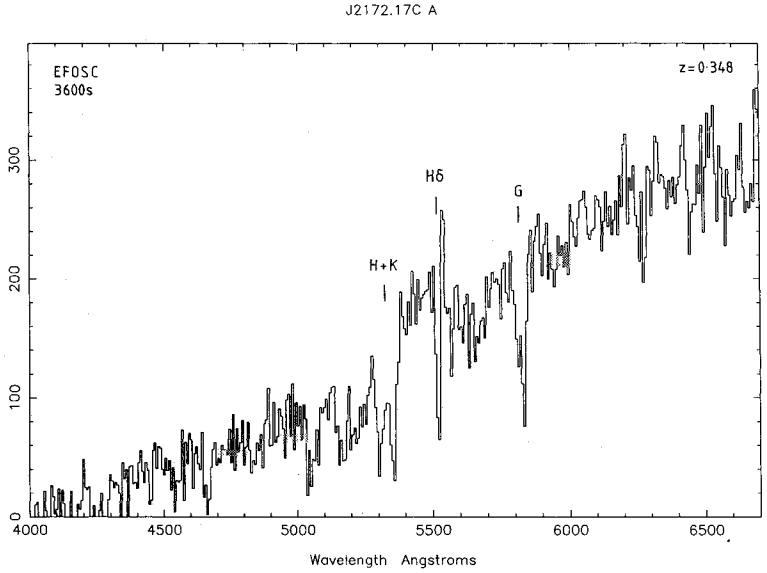

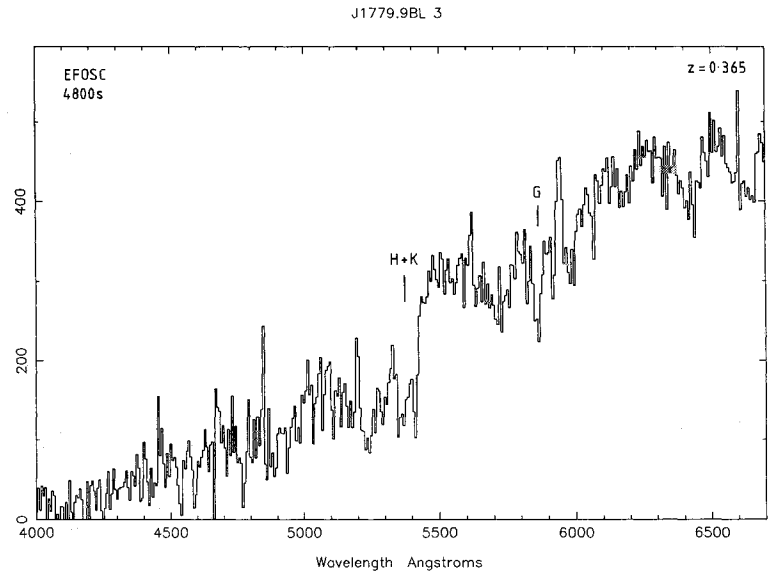

Figure 4 – *continued*

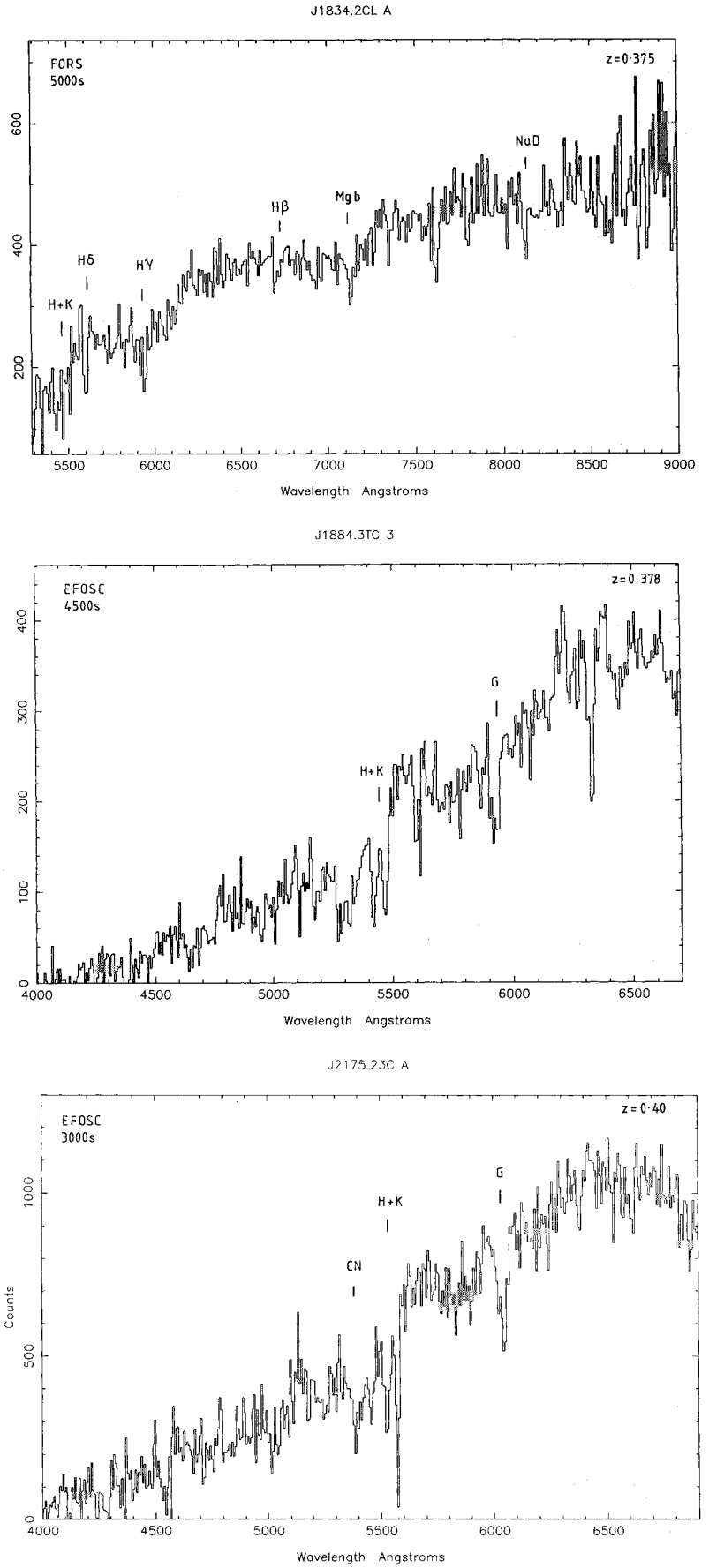

Figure 4 – *continued*

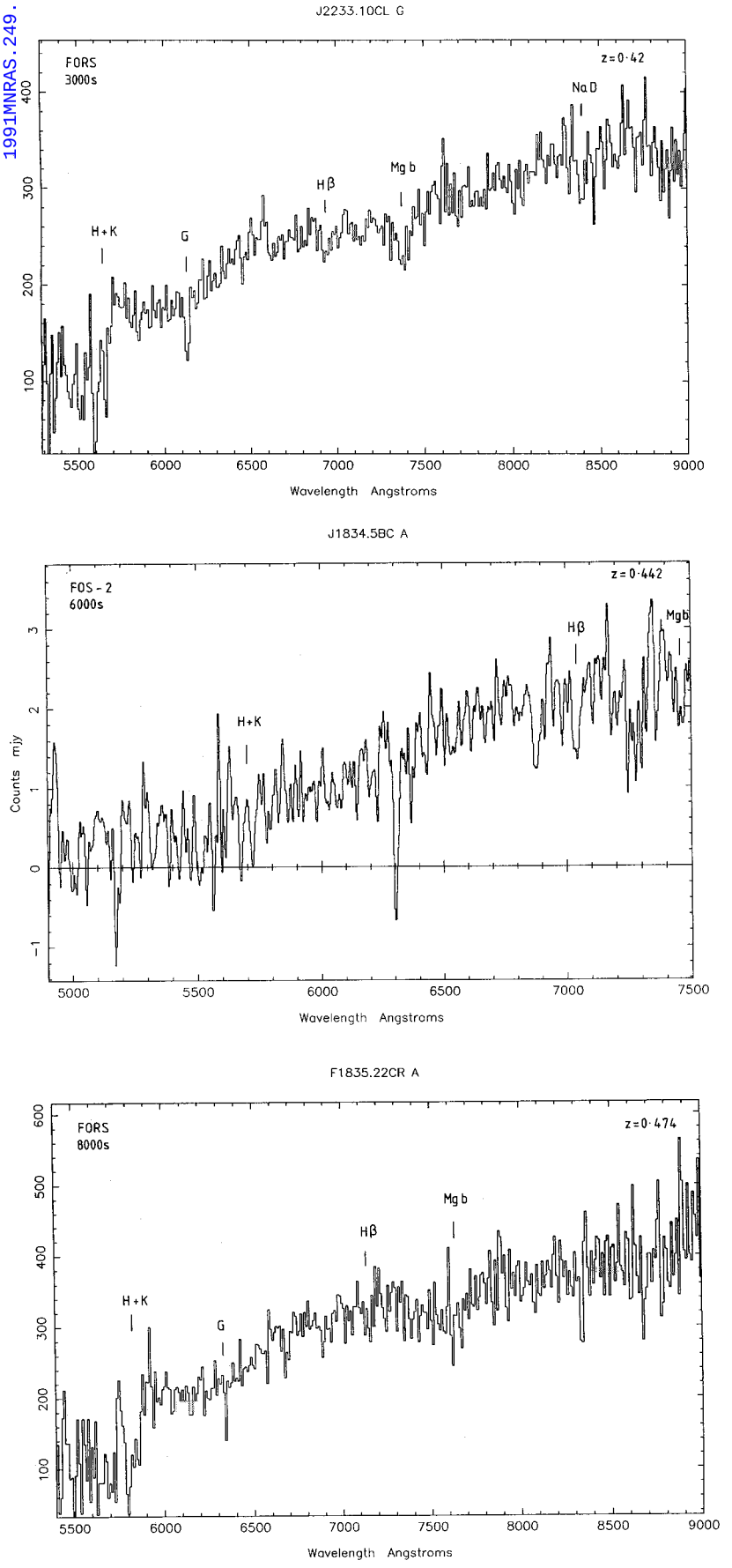

Figure 4 – *continued*

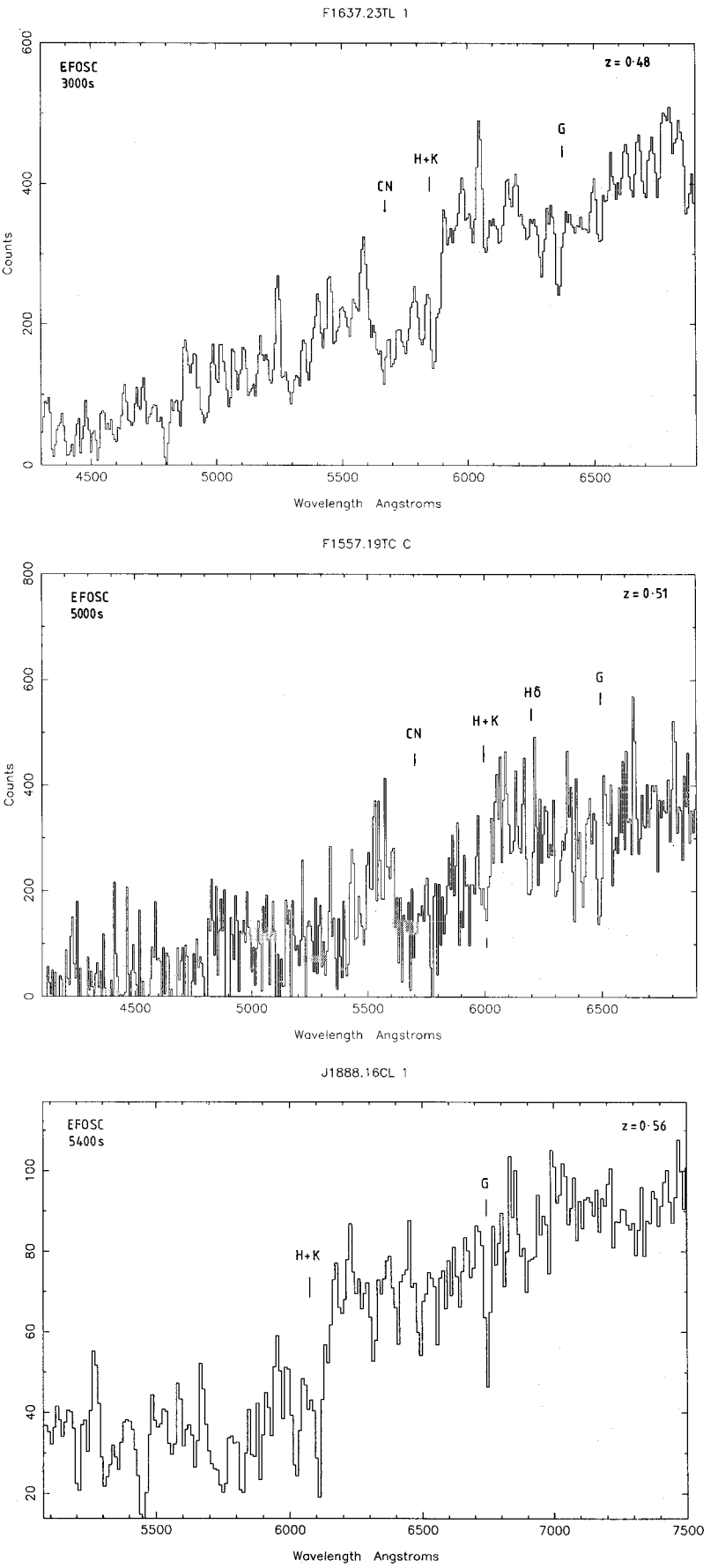

Figure 4 – *continued*

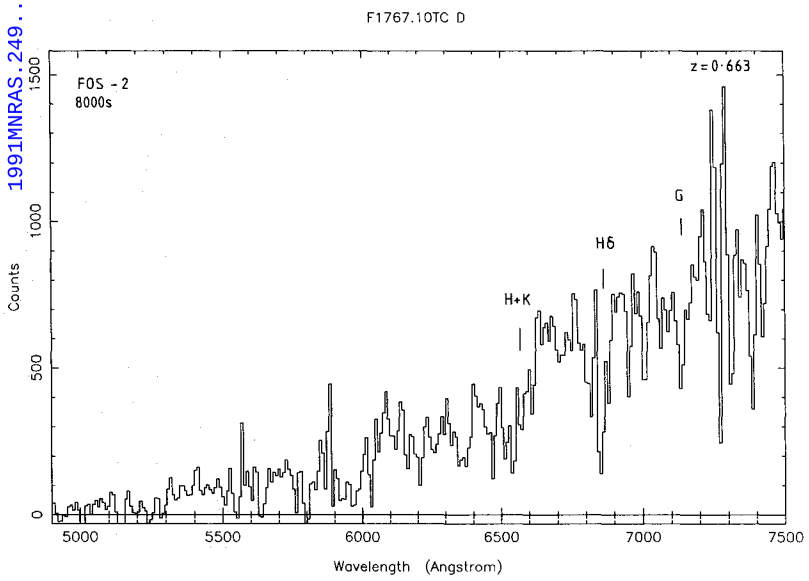

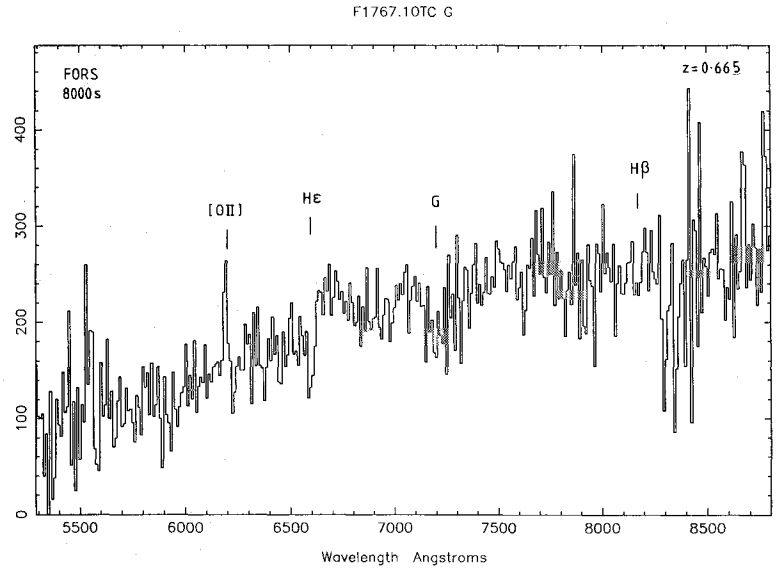

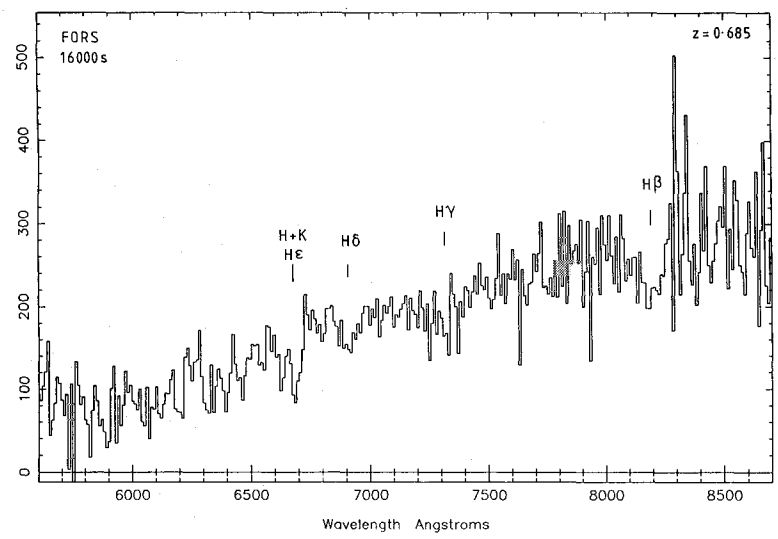

Figure 4 – *continued*

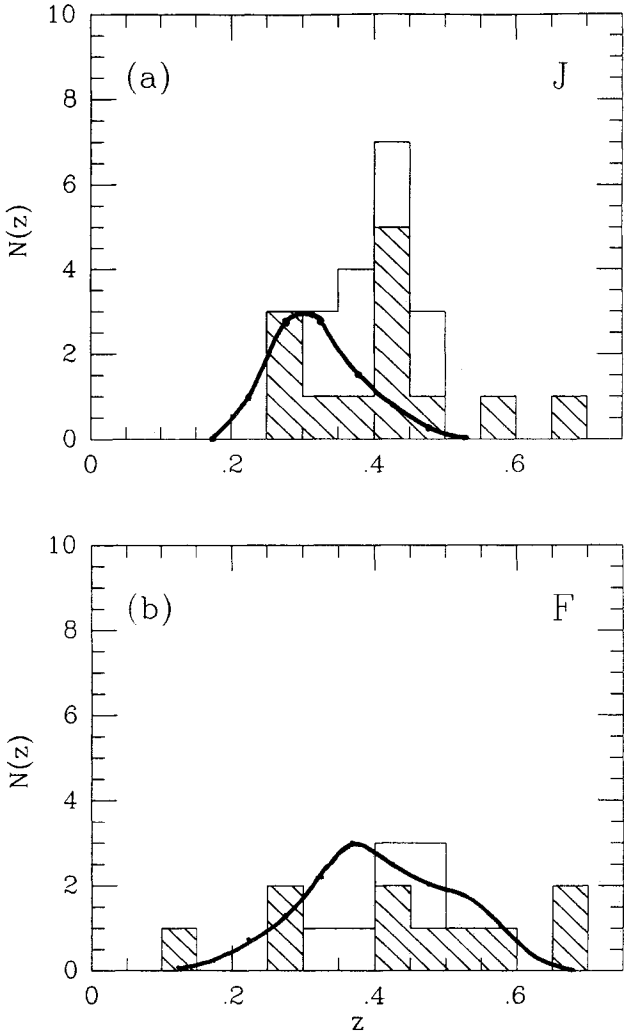

Figure 5. Redshift distribution for clusters with $\sigma_{cl} \geq 4.0$ selected in J and F (some are common to both samples). The shaded histograms refers to the complete subsample defined in the text.

image intensifier exposures covering a survey area of 11.3 deg^2.

The authors do not define precisely how their clusters were selected from this material, however, we assume a broadly similar detection technique to our own (i.e. $\sigma_{cl} \geq 3.25$) for the *photographic* portion of their survey. The AAT high-contrast technique should provide some depth advantage, but the average seeing may be different in the two samples.

In fact, if we compare the redshift distributions and surface densities, assuming a σ_{cl} limit of 3.25 for both samples (AAT and photographic Mayall) we find:

(i) the Mayall F sample contains $\simeq 1.7$ times more clusters deg^{-2} than the AAT F sample – but the sample sizes are very small and the difference is not statistically significant;

(ii) the overall Mayall sample contains a higher proportion of $z > 0.5$ clusters with the mean redshift $\bar{z} = 0.55 \pm 0.18$ significantly higher than $\bar{z} = 0.42 \pm 0.11$ for the combined AAT sample.

The second point appears to be due to the inclusion of the Mayall N plates. Beyond $z = 0.7$ there are six clusters in the GHO sample and none in the AAT sample; all were found on the Mayall N plates. The absence of any sizeable archive of AAT IV-N plates precludes an independent check on this result, but such a trend of an increasing $\bar{z}$ with effective filter wavelength is expected from the effects of the K correction in early-type systems (Fig. 3). That this trend is *not* seen when progressing from J to F in the AAT sample ($\overline{z_J} = 0.412 \pm 0.095$, $\overline{z_F} = 0.436 \pm 0.142$) suggests the larger number of J clusters is due to an additional effect.

The surface density differences may not be statistically significant but might indicate that the limiting contrast factor in the GHO sample is somewhat *lower* than $\simeq 3$ and therefore that contamination by overlapping groups could be more problematic. Unfortunately, although detailed spectroscopy has been presented for a few of the GHO clusters (Dressler & Gunn 1990), work has concentrated on a few high-redshift examples. There is no information available from which to determine the rate of contamination in the average cluster in the sample.

5.3 Evolution or foreground contamination?

Assuming that the J clusters are physical systems and that their excess number does not arise from low-redshift weak systems (Section 5.1), their high number and tendency to be found at redshifts beyond model predictions can only arise from projection effects (either by foreground groups or blue field spirals) or evolutionary effects either in the luminosity or colour of typical cluster galaxies. If evolution is responsible, the question arises as to why the effect is much more prominent in J than in F.

Already we determined (Section 4) that the incidence of interloper redshifts is satisfactorily small, and less than expected on the basis of the contrast factors across a 3 arcmin diameter. However, it is possible that clumps of foreground spirals could enhance a weak group of ellipticals raising its contrast on the J plate alone above the minimum required for inclusion in the catalogue.

To examine this effect we study the three highest-redshift ($z > 0.55$) clusters in our catalogue, noting their position in the σ_{cl}-z plane (Fig. 3). In at least one of the bands, each of these clusters lies significantly to the high redshift side of the region bounded by the non-evolution prediction. Note that the richness class 4 prediction can be ignored as far as our catalogue is concerned. These clusters have been studied in some detail.

J1888.16CL (F2262.16CL) at $z = 0.563$ – this cluster was the subject of a CCD-based photometric study by Couch *et al.* (1985). Their background-corrected galaxy count measured within 0.5 Mpc of the cluster's centre, places it at either the high-end of Abell's richness class 1 or at the low-end of class 2. Since it is based on the number of members between m_3 and $m_3 + 2.0$ mag (where m_3 is the magnitude of the third ranked member), this richness estimate is insensitive to luminosity evolution *providing* that all galaxies undergo the same amount of brightening.

Given a knowledge of the cluster's richness the exact extent of the enhancement in its contrast becomes clear (Fig. 3): what should appear as a $\sigma_{cl} \sim 1.5$ cluster in J, according to

our models, has a measured σ_{cl} of 5.3. In contrast the cluster shows only a small and barely significant σ_{cl} enhancement in *F*.

The reconciliation of this apparent excess of objects in *J* but not in *F* is a small but significant excess of blue members in comparison to expectations based on colour distributions for local clusters of similar richnesses – i.e. an effect similar to that discovered by Butcher & Oemler (1978) in intermediate-redshift samples. This is borne out by the Couch *et al.* photometry of the cluster in the *B*- and *R*-bands. A comparison of the cluster's luminosity functions in these bands with the 'non-evolved' Abell 1942 B_J and R_F luminosity functions (appropriately dimmed and *K*-shifted to $z = 0.565$) revealed that the J1888.16CL luminosity function in *R* agrees well with that of Abell 1942 after allowing for the different richness – a result consistent with the R_F contrast which matches the no-evolution prediction based on Abell 1942. An evaluation of σ_{cl} from the Couch *et al.* *R* data yields a value of 5.3, close to that derived from the HCF ($\sigma_{cl} = 5.5$).

In the blue, the J1888.16CL luminosity function is noticeably flatter in slope brightward of the 'knee', an effect which is likely due to the excess blue population boosting the bright galaxy numbers. Although the number of galaxies involved is small (~ 6), the fact that they are all relatively bright ($B \sim 22.0$–23.5) would undoubtedly raise the visibility of the cluster quite considerably. To estimate their effect in terms of σ_{cl}, we used the CCD photometry to compute the contrast the cluster would have if this component were absent.

We removed galaxies at the bright end of the J1888.16CL luminosity function until we achieved a reasonable coincidence in shape with the luminosity function of Abell 1942. By that point σ_{cl} was found to have reduced from the *B* CCD value of 5.1 [and the HCF value (see Table 3) of 5.3] to only 2.8, indicating that a blue galaxy excess is sufficient to account for the observed enhancement in the cluster contrast.

F1767.10TC at $z = 0.664$ – a multi-colour (*bVIK*) optical–infrared study undertaken by Aragón Salamanca *et al.* (in progress) provides preliminary redshift and spectral-type information for a complete sample of galaxies with $I \leq 22.5$ mag. As described by MacLaren, Ellis & Couch (1988), our technique of constructing galaxy spectral energy distributions (SEDs) via multi-band observations allows us to classify galaxies to ± 0.05 in redshift and ± 1 in Hubble type. The data convincingly confirm the reality of the cluster, with 60 per cent of the galaxies in the 3×4 arcmin^2 field of study at a redshift $z \sim 0.66$. This cluster component is dominated by objects with SEDs typical of normal present-day E/SOs; any contribution from evolved/later-type objects is less than 10 per cent.

Also of interest is the redshift distribution of the 40 per cent of galaxies that are classified as non-members. It has a broad component that one would expect from the general distribution of field galaxies along the line-of-sight to the cluster, but has superimposed upon it a narrow and quite strong peak centred at $z \sim 0.425$. Thus it appears that F1767.10TC suffers from contamination by a foreground cluster or group of galaxies. We estimate that if this system was not present, F1767.10TC would have a contrast $\sigma_{cl} \sim 5$ rather than its observed value of $\sigma_{cl} = 7.0$. Thus, in this case, contamination may explain the discrepant contrast factor reducing its true richness to $\simeq$ class 3.

J1836.23TR at $z = 0.682$ – this cluster has proven to be the most elusive in terms of confirmation and determination of a redshift. As can be seen in Table 6, spectra of at least nine objects were obtained to secure two with the same redshift. The confirmation of a cluster at $z = 0.68$ can only therefore be regarded as tentative, but it illustrates clearly the effects of contamination in the higher redshift clusters.

Of course, these three cases are insufficient to make any *general* statement about the relative roles that evolution and contamination play within our sample. However, it is interesting to note that the change from measured σ_{cl} to 'true' σ_{cl} is larger in the two *J* clusters than in the *F* cluster. More detailed work from independent studies (e.g. Butcher & Oemler 1984; Couch 1981; Couch & Newell 1984) confirms that evolution is a widespread phenomenon amongst cluster populations in our redshift range. What is also clear is that the occurrence of bluer galaxies in clusters at these earlier epochs is the result of either recent or current starburst activity going on within a subset of the cluster members (Dressler & Gunn 1982, 1983; Couch & Sharples 1987).

As an illustration of how this evolution might explain the bulk of the *J* excess without significantly affecting the *F* numbers, we have attempted to model this star formation activity and the effects it would have on the visibility of the clusters contained in our catalogue.

To quantify the effects of the starbursts seen in the distant cluster populations, we refer to the spectroscopic study by Couch & Sharples (1987, hereafter CS) of three rich clusters at $z = 0.3$. CS obtained high-quality, intermediate-resolution ($\simeq 4$ Å) spectra for 110 cluster members, a data set sufficiently large to provide statistically significant and representative information on the starburst component in distant clusters. Using the matches they obtained to their spectra [based on Bruzual's (1983) code], we can quantify the likely increase in galaxy luminosity associated with a burst.

Of the ~ 30 per cent of galaxies in the three clusters CS classified as 'blue', four out of every five were found to have recently had, or be having, a burst of star formation. The strength of the bursts, expressed in terms of the fraction of galaxy mass turned into stars, ranged from 5 up to 40 per cent. Of course, the models show the change in luminosity of a galaxy with respect to its quiescent value, which depends critically on both the strength and the duration of the burst. By averaging over the CS observed distribution of burst strength and age, we can estimate the mean overall brightening that can typically be attributed to this component of the distant cluster populations, assuming that these three clusters are representative of those in our new cluster sample. We do this for both our *J* and *F* bands which, at the redshifts of our clusters, imply rest wavelengths in the ultraviolet and blue–visual regions, respectively. The rest wavelength coverage is particularly important here since the biggest increase in brightness to result from a burst is seen at ultraviolet wavelengths, with changes at longer wavelengths being considerably smaller. When placed at $z = 0.45$, a redshift representative of our cluster sample, the CS population of burst- and post-burst galaxies (i.e. those they classified as Type 1 or Type 3) would, on average, appear to have

brightened by ~ 1.8 mag in J and ~ 0.6 mag in F with respect to their quiescent-state luminosities. As expected, such short-term evolutionary effects have a much greater impact on the J-band than on the F-band, as required to explain the observed/predicted cluster number ratios discussed earlier.

The net effect of this brightening in terms of cluster visibility was determined by repeating the (σ_{cl}, z) calculations with appropriate corrections to the cluster luminosity functions at redshifts 0.5, 0.6 and 0.7. Assuming a bursting proportion of 30 per cent, we calculated the likely increase in σ_{cl} for selection in J and F (see arrows in Fig. 3). As expected, the effect is much stronger in J than F and thus could explain the discrepancy between our observed and predicted numbers in that pass-band, as well as the extended redshift distribution. The effect would also partly explain the position of clusters such as J1888.16CL in the J (σ_{cl}, z) diagram.

To revise the no-evolution cluster number predictions to account for the effects of burst activity is difficult, however, since the CS observations provide us with only a 'snapshot' of the burst phase in distant clusters. In reality we expect a spread amongst the clusters indicative of how far their galaxies have proceeded through the burst cycle. Those whose populations we catch earlier in the burst phase will have an even higher contrast while those caught later will have a lower contrast. Unfortunately, with the spectroscopic and photometric information accumulated for distant cluster populations so far, it has not been possible to establish exactly what cluster property determines the epoch at which the burst activity begins (Dressler & Gunn 1990). Despite this, our predictions have served a useful purpose in providing an indication of the size of the effects involved and, most importantly, in demonstrating their strong pass-band dependence.

This calculation simply shows that short-term star formation of the kind known to exist in distant clusters (CS; Dressler & Gunn 1982, 1983) can explain, under the 'evolutionary' heading of Section 3.2, how the effect is predominantly in the J samples without significantly distorting the mean redshift of that sample with respect to that selected in F. However, it does not necessarily mean that contamination is not also important, and indeed could be the dominant effect.

We can place some limit on contamination by considering in Fig. 6 the redshift distribution of the interloping galaxies found in the course of our cluster redshift observations. If these galaxies had been drawn from the general field population down to the faintest magnitudes at which the objects were observed spectroscopically ($F \sim 22$, $J \sim 23$), then we would expect a $N(z)$ distribution indicated by the solid curve (*cf.* Colless *et al.* 1990). Clearly this is not consistent with our observed distribution which is skewed significantly towards higher redshifts. Indeed, the interloper sample has a surprisingly small number of emission-line galaxies which are characteristic of those found in field redshift surveys at faint magnitudes. One interpretation of this discrepancy is that the clusters are principally contaminated, not by field galaxies, *but by other clusters or groups* along the line-of-sight. In support of this, we note that the excess interloper population, i.e. those with redshifts in excess of what would be expected for a random field sample, has a similar mean redshift to the tail of 'extra' galaxies in the J cluster sample. However, it is still surprising that there is no distortion of the redshift distribution in the F sample, although the samples are admittedly small.

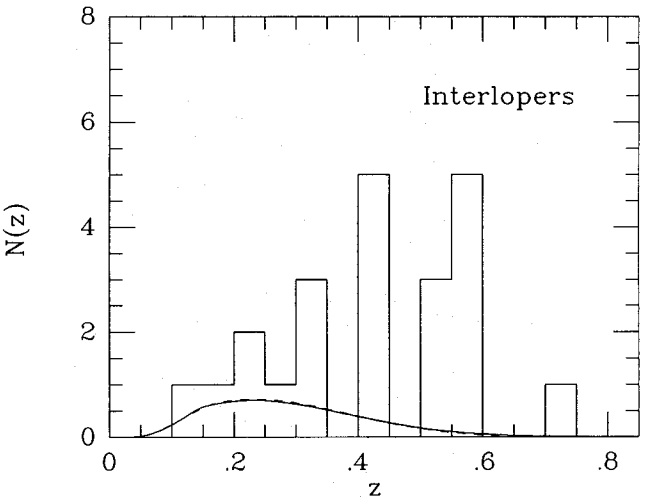

Figure 6. Redshift distribution for interlopers (non-cluster members) – both J and F samples – compared with the overall redshift distribution for field samples limited at $J = 23$ (solid line) and $F = 22$ (dashed line) consistent with the field surveys of Colless *et al.* (1990).

Of course, the issue of contamination versus evolution can only be properly addressed on a cluster-by-cluster basis with the acquisition of detailed membership statistics. We are tackling this task for a number of clusters in our catalogue via multi-object spectroscopic observations as well as our multi-colour intermediate-band imaging technique. This approach, based on a uniformly selected set of clusters which our catalogue provides, will allow us to attack the central question of the physical processes governing cluster galaxy evolution at past epochs.

Finally, we make some remarks on the prospects of searching for higher-redshift clusters. The trends observed in mean redshift, $\bar{z}$, with pass-band suggest numerous selection biases. None of the following remarks is especially secure, but overall the comments are useful in defining a strategy for finding higher-redshift clusters.

In our own catalogue, the J survey is sensitive to rich clusters whose galaxies are undergoing bursts of star formation as well as to some overlapping groups. Our F sample is less affected by such biases and may generally pick up galaxy samples whose bursts terminated some time ago, or where the activity is less extreme. GHO found more high-redshift clusters than we did probably by selecting in the Mayall N-band, but if bursting is a phenomenon that continued over a wide range in epochs, one might expect to see somewhat deeper in F than is actually the case. The sample of clusters with $z > 0.5$ is too small to warrant detailed modelling. What *is* apparent, however, is that for those of us wishing to use distant cluster catalogues to study galaxy evolution there are severe dangers in *any* optical selection.

At 1–2 μm the spectral energy distributions of most galaxy types converge regardless of the nature and amount of star formation. Accordingly, imaging surveys at K offer the best prospects for furthering this work. Current technology

cannot offer the panoramic fields required. The current AAT sample was gleaned from a 51 deg^2 area which would require $\sim 10^5$ images with current infrared arrays!

A more immediate proposition is the use of X-ray data, particularly from the *ROSAT* survey (Trümper 1984). By selecting clusters at wavelengths where the radiation is largely unrelated to the galaxy properties, one might hope to be immune to the various difficulties mentioned above. The prospects of evolution in the X-ray luminosity must also be considered however, and thus the absence of high-redshift X-ray clusters need not necessarily imply a recent growth of clustering as predicted in certain cosmological models (Frenk *et al.* 1990).

6 CONCLUSIONS

Summarizing our main achievements and results.

(i) We have tested the suitability of high-contrast derivatives of AAT prime focus plates for finding distant galaxy clusters by comparing object catalogues found by eye on these films with those determined by measuring machine photometry of the original plates. Our tests show excellent visibility and reproducibility with effective limiting magnitudes for the J and F films of $b_J \simeq 24.4$ and $r_F \simeq 22.9$ respectively. The variation from film to film is about $\simeq 0.2$–0.3 mag.

(ii) Using a selection of 55 AAT films with sky-limiting exposures and reasonable seeing, we tabulate 112 faint cluster candidates identified by the application of a simple *contrast* criterion, σ_{cl}, which measures the cluster excess within a 3 arcmin diameter against the rms variation in the background field on the same film. Candidates are listed down to $\sigma_{cl} = 2.0$.

(iii) Correlating our list with catalogues based on the Schmidt telescope searches conducted by Abell and co-workers confirms that the bulk of our candidates should be more distant, i.e. $z > 0.2$.

(iv) We have simulated the appearance of typical 1 deg^2 fields using recent estimates of the volume density of Abell clusters of different richness types and superimposing a field population with the fluctuations observed. By applying the same search criteria to the simulated fields we can check for the omission of clusters and the inclusion of unphysical clusters as a function of the contrast σ_{cl}. We find that spurious effects caused by fluctuations in the field counts and undetected clusters become significant only below $\sigma_{cl} = 3.25$ with undetected clusters occurring at a rate dependent on the central concentration. Accordingly we adopt this as a completeness limit for the catalogue.

(v) Assuming no evolution in galaxy properties or comoving cluster number densities, our simulations predict about the observed number of F clusters above our completeness limit, but too few J clusters are predicted by a significant margin. This excess of J clusters, which also appear to be at higher redshifts than predicted, could arise from a population of low-redshift, spiral-rich groups (either in contamination or independent of the F cluster population) or from galaxy evolution associated with the Butcher–Oemler effect.

(vi) To check the origin of the observed excess of blue clusters, we have measured redshifts for 29 of the 44 clusters with $\sigma_{cl} > 4.0$. Although not a complete sample, a sub-sample of clusters in 16 fields is spectroscopically complete and this allows us to normalize for absolute predictions. Our spectroscopy confirms the reality of the clusters with $\sigma_{cl} > 4.0$ (only 1/29 might be spurious) and reveals a redshift range for both J and F samples similar to that expected from the simulations.

(vii) A comparison with the northern cluster sample of Gunn *et al.* (1986) is rendered difficult by the absence of clear selection criteria in that work. Assuming they adopted similar criteria to ourselves for the photographic material in their survey, we find roughly the same surface densities but their mean redshift, $\bar{z}$, is strongly dependent on pass-band – in contrast to that found in the AAT survey. The greater depth in their catalogue appears to result from the inclusion of N plates which can be understood if the bulk of the high-redshift clusters they find are prominent in early-type red galaxies.

(viii) A detailed examination of the highest-redshift clusters confirms the likelihood of both possible causes for the excess of blue clusters – projections from foreground spiral-rich groups and colour evolution associated with star formation activity within the cluster environment. We demonstrate how bursts of star formation in a subset of cluster galaxies could dramatically transform the J contrast leaving the F contrast largely unaffected – in agreement with the basic trend observed. Our spectroscopic sample is too small to quantify the extent to which evolution dominates projection effects.

(ix) The variation of galaxy luminosity and colour as a function of time in the rich cluster environment implies worrying selection effects will be present in any search for distant clusters which relies on the detection of galaxy light at optical wavelengths. This is especially so if a main application of the distant cluster catalogue is to study galaxy evolution. Only with the advent of wide-field infrared (2 μm imaging) or X-ray selected samples, might such biases be overcome and a sensible estimate of possible evolution in galaxy properties or in cluster number densities be found.

ACKNOWLEDGMENTS

This project owes much to the dedication of the staff at the Anglo–Australian Telescope, particularly its former Director, Don Morton, who encouraged the formation and exploitation of the photographic archive on which this cluster sample is based. We also thank the APM and COSMOS teams, particularly Ed Kibblewhite and Harvey MacGillivray, for their eagerness to rationalize the question of the applicability of HCFs for faint object astronomy. For the spectroscopy we thank Ian Parry and Gordon Robertson for the basis of the extraction software used, and David Allen, Jeremy Allington-Smith, Keith Taylor and Sandro D'Odorico for their generous assistance with the various instruments used. Finally, we acknowledge encouragement from Jim Gunn and John Hoessel and useful discussions with John Lucey, Ray Sharples and Carlos Frenk.

REFERENCES

Abell, G. O., 1958. *Astrophys. J. Suppl.*, **3**, 211.

Abell, G. O., Corwin, H. G. & Olowin, R. P., 1989. *Astrophys. J. Suppl.*, **70**, 1.

Allington-Smith, J. R., Breare, J. M., Ellis, R. S., Gray, P. M. & Worswick, S. P., 1988. *Gemini,* **No. 19,** 2.
Bahcall, N. A., 1977. *Astrophys. J.,* **217,** L77.
Breare, J. M. *et al.*, 1987. *Mon. Not. R. astr. Soc.,* **227,** 909.
Broadhurst, T. J., Ellis, R. S., Koo, D. C. & Szalay, A. S., 1990. *Nature,* **343,** 726.
Bruzual, G., 1983. *Astrophys. J.,* **273,** 105.
Butcher, H. & Oemler, A., 1978. *Astrophys. J.,* **226,** 559.
Butcher, H. & Oemler, A., 1984. *Astrophys. J.,* **285,** 426.
Chincarini, G., 1988. In: *Towards Understanding Galaxies at Large Redshifts,* p. 217, eds Kron, R. G. & Renzini, A., Kluwer, Dordrecht.
Colless, M. M., Ellis, R. S., Taylor, K. & Hook, R. N., 1990. *Mon. Not. R. astr. Soc.,* **244,** 408.
Couch, W. J., 1981. *PhD thesis,* Australian National University.
Couch, W. J., Ellis, R. S., Kibblewhite, E. J., Malin, D. F. & Godwin, J., 1984. *Mon. Not. R. astr. Soc.,* **209,** 307.
Couch, W. J., Ellis, R. S. & Malin, D. F., 1989. In: *The World of Galaxies,* p. 25, eds Corwin, H. G. & Bottinelli, L., Springer-Verlag, Berlin.
Couch, W. J. & Newell, E. B., 1984. *Astrophys. J. Suppl.,* **56,** 153.
Couch, W. J., Shanks, T. & Pence, W. J., 1985. *Mon. Not. R. astr. Soc.,* **213,** 215.
Couch, W. J. & Sharples, R. M., 1987. *Mon. Not. R. astr. Soc.,* **229,** 423 (CS).
Dressler, A. & Gunn, J. E., 1982. *Astrophys. J.,* **263,** 563.
Dressler, A. & Gunn, J. E., 1983. *Astrophys. J.,* **270,** 7.
Dressler, A. & Gunn, J. E., 1990. In: *Hubble Centennial Symposium: Evolution of Galaxies,* p. 200, ed. Kron, R. G., ASP Conference Series.
Ellis, R. S., 1987. In: *Observational Cosmology, IAU Symp. 124,* p. 367, Burbidge, G. & Fang, Z., Reidel, Dordrecht.
Ellis, R. S., 1988. In: *Towards Understanding Galaxies at High Redshift,* p. 147, eds Kron, R. & Renzini, A., Kluwer, Dordrecht.
Ellis, R. S. & Parry, I. R., 1988. In: *Instrumentation for Ground-Based Astronomy,* p. 192, ed. Robinson, L., Springer-Verlag, Berlin.
Frenk, C. C., White, S. D. M., Efstathiou, G. & Davis, M., 1990. *Astrophys. J.,* **351,** 10.
Gunn, J. E., Hoessel, J. & Oke, J. B., 1986. *Astrophys. J.,* **306,** 30 (GHO).
Jones, L. R., Fong, R., Shanks, T., Ellis, R. S. & Peterson, B. A., 1991. *Mon. Not. R. astr. Soc.,* **249,** 481.
Kibblewhite, E. J., 1980. *APM Facility Manual,* Institute of Astronomy, Cambridge.
King, C. R. & Ellis, R. S., 1985. *Astrophys. J.,* **288,** 456.
Koo, D. C., 1981. *Astrophys. J.,* **251,** L75.
Koo, D. C. & Kron, R., 1988. In: *Towards Understanding Galaxies at High Redshift,* p. 209, eds Kron, R. & Renzini, A., Kluwer, Dordrecht.
Leir, J. & van den Bergh, S., 1977. *Astrophys. J. Suppl.,* **34,** 383.
Lucey, J. R., 1983. *Mon. Not. R. astr. Soc.,* **204,** 33.
MacLaren, I., 1987. *PhD thesis,* University of Durham.
MacLaren, I., Ellis, R. S. & Couch, W. J., 1988. *Mon. Not. R. astr. Soc.,* **230,** 249.
Malin, D. F., 1978. *Nature,* **276,** 591.
Malin, D. F. & Carter, D., 1980. *Nature,* **285,** 643.
Peterson, B. A., Ellis, R. S., Kibblewhite, E. J., Bridgeland, M. T., Hooley, T. & Horne, D., 1979. *Astrophys. J.,* **233,** L109.
Robertson, J. G., 1986. *Publs astr. Soc. Pacif.,* **98,** 1220.
Shanks, T., Stevenson, P. R. F., Fong, R. & MacGillivray, H. T., 1984. *Mon. Not. R. astr. Soc.,* **206,** 767.
Stobie, R. S., Smith, G. M., Lutz, R. K. & Martin, R., 1979. In: *Image Processing in Astronomy,* ed. Capaccioli, M., Trieste.
Trümper, J., 1984. *Physica Scripta,* **T7,** 209.
Zwicky, F., Herzog, E., Wild, P., Karpowicz, M., Kowal, C. T., 1961–1968. *Catalogue of Galaxies and Clusters of Galaxies,* 6 volumes, Caltech, Pasadena.